

SECURITY CLASSIFICATION OF THIS PAGE (When Data Entered)

REPORT DOCUMENTATION PAGE		READ INSTRUCTIONS BEFORE COMPLETING FORM
1. REPORT NUMBER NSWC/WOL/TR 76-39	2. GOVT ACCESSION NO.	3. RECIPIENT'S CATALOG NUMBER
4. TITLE (and Subtitle) "Scattering of Electromagnetic Radiation by Apertures: XIII. The Electric Field in the Slot Near the TM_{01} Cutoff for a Longitudinally Narrow Slotted Conducting Cylinder."		5. TYPE OF REPORT & PERIOD COVERED Topical
		6. PERFORMING ORG. REPORT NUMBER
7. AUTHOR(s) L. F. Libelo, NSWC/WOL, R. S. Dunbar, SUNYA, and J. N. Bombar dt, HDL (on leave to Princeton University)		8. CONTRACT OR GRANT NUMBER(s) N60921-75C-0131
9. PERFORMING ORGANIZATION NAME AND ADDRESS Naval Surface Weapons Center White Oak Laboratory Silver Spring, Maryland 20910		10. PROGRAM ELEMENT, PROJECT, TASK AREA & WORK UNIT NUMBERS NMAT 03L-000/ZR011-01-01 DNA: R99QAXEB088 HDL: E052E6 Subtask EB088
11. CONTROLLING OFFICE NAME AND ADDRESS		12. REPORT DATE April 1976
		13. NUMBER OF PAGES 81
14. MONITORING AGENCY NAME & ADDRESS (if different from Controlling Office)		15. SECURITY CLASS. (of this report) UNCLASSIFIED
		15a. DECLASSIFICATION/DOWNGRADING SCHEDULE
16. DISTRIBUTION STATEMENT (of this Report) Approved for public release, distribution unlimited.		
17. DISTRIBUTION STATEMENT (of the abstract entered in Block 20, if different from Report)		
18. SUPPLEMENTARY NOTES The effort was funded jointly by the Defense Nuclear Agency, NSWC/WOL under the IR program and the State University of New York at Albany with partial support from NSWC/WOL under contract N60921-75-C-0131. Work was performed in collaboration with HDL and SUNY at Albany, N.Y.		
19. KEY WORDS (Continue on reverse side if necessary and identify by block number) Electromagnetic Diffraction Narrow Axial Slots in Cylinders E-polarized Incident Radiation Near TM_{01} Effects of Variation of Cylinder Parameters in Measured Field at Slot Center		
20. ABSTRACT (Continue on reverse side if necessary and identify by block number) The fields for an infinite slotted circular cylinder are derived for arbitrary incidence and polarization. For a narrow slot and E-polarized incident radiation a large field amplitude is shown to occur in the slot at non-resonant frequencies. For the lowest modes the resonance line in the slot is calculated for a very narrow aperture at normal, symmetric incidence. Measurements in the slot of		

DD FORM 1 JAN 73 1473

EDITION OF 1 NOV 65 IS OBSOLETE
S/N 0102-014-6601

UNCLASSIFIED

SECURITY CLASSIFICATION OF THIS PAGE (When Data Entered)

UNCLASSIFIED

SECURITY CLASSIFICATION OF THIS PAGE(When Data Entered)

a finite cylinder are shown along with the effects of varying slot angle, slot length and cylinder length.

UNCLASSIFIED

SECURITY CLASSIFICATION OF THIS PAGE(When Data Entered)

20 April 1976

NSWC/WOL/TR 76-39

SCATTERING OF ELECTROMAGNETIC RADIATION BY APERTURES: XIII. THE ELECTRIC FIELD IN THE SLOT NEAR THE TM_{01} CUTOFF FOR A LONGITUDINALLY NARROW SLOTTED CONDUCTING CYLINDER.

This report contains the results of a combined theoretical and experimental investigation into an electromagnetic diffraction problem. The study was performed jointly in the Physics Department at the State University of New York at Albany, N.Y., at the Naval Surface Weapons Center/White Oak and at the U. S. Army, Harry Diamond Laboratories, Adelphi, Md. At the State University of New York the efforts were partially supported by NSWC/WOL under contract N60921-75-C-0131. At NSWC/WOL the effort was supported partly by the Defense Nuclear Agency under Task DNA-R99QAXEB088 and partly by the Independent Research Program (Task Number MAT-03L-000/ZR011-01-01). At HDL the effort was supported by the Defense Nuclear Agency under Task DNA EB088-52. This document is for information only.



LEMMUEL L. HILL

TABLE OF CONTENTS

	Page
LIST OF FIGURES	3
I. INTRODUCTION	5
II. THEORY	11
1. Arbitrary Incidence	11
2. E-polarization and Arbitrary Incidence in Plane of Symmetry Through the Slot	28
3. Symmetric, Normal Incidence of E-polarized Radiation	43
III. THE EXPERIMENTAL METHOD	47
IV. EXPERIMENTAL RESULTS IN THE TM_{01} REGION	52
V. SUMMARY	77
LIST OF REFERENCES	80

LIST OF FIGURES

Figure	Title	Page
1	Geometry of Arbitrary Incident Linearly Polarized Plane Wave Irradiating Longitudinally Slotted Circular Cylinder	13
2	Electric Field Amplitude at Center of Slot in Circular Cylinder for $\phi_0=6^\circ$ Slot and E-polarized Radiation at Normal Symmetric Incidence Near the TM_{01} and TM_{11} Circular Waveguide Modes	45
3	Principal Components of Measuring System and Their Interconnections	48
4	Detailed Illustration of the Electric Field Probe	51
5	Measured Amplitude of Electric Field at Slot Center Versus γ for Various Slot Angles. The Theoretical Prediction for $\phi_0=6^\circ$ is Shown for Comparison with the Infinite Cylinder	53
6	The Measured Value of γ At Peak Maximum versus Slot Angle Using the Five-Foot (152.4cm) Long Slotted Cylinder	56
7	Measured Linewidth of the Amplitude of the Longitudinal Electric Field at the Center of the Slot as a Function of Slot Angle	57
8	Measured Peak Amplitude of Electric Field at the Slot Center as a Function of Slot Angle for 5 ft (152.4cm) Long Cylinder with Full Length Axial Slot	59
9	Measured Value of γ at Peak Versus Slot Length in Units of Wavelength at Peak for Various Slot Angles	61
10	Measured Linewidth Versus Slot Length in units of Wavelength at the Peak Value of Slot Field for Various Slot Angles	63
11	Measured Peak Amplitude of Electric Field at Slot Center Versus Slot Length in Units of Peak Wavelength for Various Slot Angles	65

LIST OF FIGURES (CONT.)

Figure	Title	Page
12	Measured Values of γ at Peak Versus Cylinder Length in Units of Reference Cylinder Length $L_o=5$ ft.(152.4cm) for Various Slot Angles	68
13	Measured Linewidth as a Function of Cylinder Length L_c in Units of the Reference Cylinder Length $L_o=5$ ft.(152.4cm) for Various Slot Angles	70
14	Peak Amplitude of Electric Field at Slot Center Versus Cylinder Length L_c in Units of Reference Cylinder Length $L_o=5$ ft.(152.4cm) for Various Slot Angles	71
15	Measured Values of γ at Peak Aperture Field Versus Slot Angle for Various Slot Lengths L_s in Units of Reference Length $L_o=5$ ft.(152.4cm)	73
16	Measured Values of γ at Peak Slot Field Versus Slot Angle for Various Cylinder Lengths L_c in Units of Reference Cylinder Length $L_o=5$ ft.(152.4cm)	74

I. INTRODUCTION

Over the past few years we have issued a number of reports¹⁻⁴ on the results of our investigations into the scattering characteristics of axially slotted conducting circular cylinders subject to irradiation by linearly polarized, plane, monochromatic electromagnetic waves. The only situation omitted from these reports is that corresponding to the presence of a very narrow slot in the conducting cylinder. We have in past publications declared that this case was of sufficient interest to merit a report of its own. In this paper we shall consider one phase of this problem and shall in the course of these considerations demonstrate the significance of this particular problem. In the next section we develop the theory for the case of arbitrary incidence on the slotted conducting cylinder. At the end of that development we shall point out a condition under which we have a potentially hazardous degree of coupling of the incident energy through the narrow slot. Following this we consider the seemingly innocuous case of radiation polarized parallel to the

-
1. J. N. Bombar dt & L. F. Libelo, "S.E.R.A. III. An Alternative Integral Equation with Analytic Kernels For the Slotted Cylinder Problem," HDL-TR-1588 Harry Diamond Labs., Washington, D.C., August 1972.
 2. J. N. Bombar dt & L. F. Libelo, "S.E.R.A. IV. Slotted Cylinders and Cylindrical Strips In the Rayleigh Limit," HDLTR-1607 Harry Diamond Labs., Washington, D.C., August 1972.
 3. J. N. Bombar dt & L. F. Libelo, "S.E.R.A. V. Surface Current, Tangential Aperture Electric Field and Back-Scattering Cross-Section For the Axially Slotted Cylinder at Normal, Symmetric Incidence," NSWC/WOL/TR 75-39 April 1975.
 4. L. F. Libelo, A. G. Henney, J. N. Bombar dt & F. S. Libelo, "S.E.R.A. X. The Axially Slotted Infinite Cylinder-Internal and Near Aperture Fields. Surface Current, Aperture Field and B.S.C.S. For Intermediate Slot Angles," NSWC/WOL/TR 75-162 January 1976.

cylinder axis and incident normal to that axis and symmetric with respect to the narrow slot. We then proceed in part III to discuss the experimental technique we followed to investigate whether or not this critical degree of coupling in the theoretical case of an infinitely long cylinder also obtains for a real cylinder of finite length but still possessing what appears to be characteristics of the infinite cylinder. In part IV we compare our experimental results with our theoretical predictions for the infinite cylinder. We further show experimental results obtained by varying the parameters inherent in the diffraction problem. The final part of this report is a discussion of the results obtained.

Before proceeding to the development of the formal expressions we first present a brief review of the history of this particular problem. This will help to cast the diffraction problem in its proper perspective. Sommerfeld⁵ was apparently the first person to report on the diffraction of plane electromagnetic waves by a perfectly conducting circular infinite cylinder containing a full length axial slot. He formulated the solution for the internal and the external fields in terms of series expansions. Only in the limit where the slot arclength is small in comparison to the wavelength of the incident radiation did he attempt to actually evaluate the coefficients in the series expansions for the fields. Using the method of least squares he managed to derive analytic expressions

5. A. Sommerfeld, "Partial Differential Equations In Physics," pp. 29, 159 Academic Press Inc. New York 1949.

for the coefficients in this asymptotic limit. Unfortunately he made no attempt to actually evaluate numerically these series expansion coefficients which explicitly give the diffracted fields. Morse and Feshbach⁶ treated the same problem using approximate methods. They also assumed series expansions for the fields. In their approach the unknown series expansion coefficients were expressed in terms of an integral of the unknown electric field over the slot. Approximate solution of this integral equation was achieved by their assuming that the distribution of the electric field over the slot in the axially slotted cylinder, is proportional to the electrostatic field distribution over an infinite slot in an infinite plane. We have shown that^{3,4} this represents a rather good qualitative approximation to the slot electric field in the case of the incident radiation polarized parallel to the cylinder axis. Morse and Feshbach were able to derive an analytic result for the proportionality constant at the midpoint of the slot. However, we are again unfortunate in that they failed to furnish any numerical or experimental results for the expansion coefficients which explicitly determine the diffracted fields. Hayashi^{7,8} published another method for the

-
6. P. M. Morse and H. Feshbach, "Methods of Theoretical Physics, Part II," p. 1387-1398 McGraw Hill Book Co. Inc., New York 1953.
 3. S.E.R.A. V. J. N. Bombardt and L. F. Libelo, Ibid.
 4. S.E.R.A. X. L. F. Libelo, A. G. Henney and F. S. Libelo, Ibid.
 7. Y. Hayashi, "Electromagnetic Field In a Domain Bounded by a Coaxial Circular Cylinder With Slots," Proc. Japan Acad. 40, 305 (1964).
 8. Y. Hayashi, "On Some Singular Integral Equations I," Proc. Japan Acad. 40, 323 (1964).

formal solution of diffraction at a plane wave by a longitudinally slotted infinite circular cylinder. Again he did not explicitly evaluate the fields in the problem. Barakat and Levin⁹ restudied the problem at normal symmetric incidence of plane monochromatic radiation polarized with the incident electric field parallel to the cylinder axis. They used the least squares method of Sommerfeld. For circumference to wavelength ratios of 0.25, 0.50, 0.75 and 1.00 they calculated the coefficients for three term electric field expansions inside and outside the cylinder containing a 10° slot. It should be noted that these circumference to wavelength ratios are considerably beyond the cutoff of the lowest circular waveguide mode which lies at just beyond 2.404. They indicated that for values of the ratio greater than about unity the Sommerfeld perturbation method becomes numerically unreliable. They further concluded that the method would yield reliable results only in the strictest Rayleigh limit of very small slots and very long wavelength. Unfortunately this prohibits applying the Sommerfeld least squares technique to the study of narrow slot characteristics very close to the circular waveguide resonances. Applying the Riemann-Hilbert method¹⁰ Koshparënok and Shestopalov¹¹ approximately solved in analytic form the diffrac-

-
9. R. Barakat and E. Levin, "Diffraction of Plane Electromagnetic Waves by a Perfectly Conducting Cylindrical Lamina," Jour. Opt. Soc. Amer. 54, 1089 (1964).
 10. V. P. Shestopalov, "The Method of the Riemann-Hilbert Problem In the Theory of Diffraction Propagation of Electromagnetic Waves," (Untranslated from the Russian) Izd. KhGU, Kharkov (1971).
 11. V. N. Koshparënok and V. P. Shestopalov, "Diffraction of a Plane Electromagnetic Wave by a Circular Cylinder with a Longitudinal Slot," Zh. Vychisl. Mat. i Mat. Fiz. 11, 721 (1971).

tion problem for a plane wave irradiating an infinite circular cylinder containing a narrow full length axial slot. They considered only the case where in the incident radiation the wave vector has components only along the cylinder axis and in the plane through that axis and parallel to the slot edges. The effect of radiation at incidence off the cylinder axis was studied near the circular waveguide resonances. In the next section this property will be presented in detail. They showed that even for a "non-resonant" frequency for the incident radiation resonant excitation could theoretically be achieved by appropriately choosing the incident direction of the electromagnetic wave. It should be noted that they did not perform experiments to investigate these important theoretical predictions. We finally cite another important study. Koshparënok et. al.¹² extended the previous study to the same problem with emphasis now on H-polarized radiation i.e. the incident H-field is polarized along the slotted cylinder axis. In this investigation calculations were carried out by the Riemann-Hilbert method for narrow slots. Furthermore, they experimentally investigated, using the 3.9-5.2mm band, the excitation of the TE modes in a long circular cylinder with a narrow slot. They were unable in their program of measurement to investigate the TM modes for the slotted cylinder although they did study the TE modes excited by incident E-polarized radiation. In their paper we see the first empirical results obtained for the

12. V. N. Koshparënok, G. G. Polovnikov and V. P. Shestopalov, "Resonant Excitation of a Circular Cylinder with a Longitudinal Slot By a Plane Wave," Sov. Phys.-Tech. Phys. 17, 1630 (1973).

dependence of the resonant excitation in narrowly slotted circular cylinders by off normal incidence of radiation at non-resonant frequencies. In a subsequent paper we shall present detailed results of our program of measurement of the effects of H-polarized incident radiation on a narrow slotted cylinder.

One final introductory comment should be made. Our theoretical results near resonance that we present below were calculations made by a high order method of moments application. In S.E.R.A. V.³ we described this numerical method in adequate detail and shall not explicitly repeat it here.

3. J. N. Bombardt and L. F. Libelo, S.E.R.A. V., Ibid.

II. THEORY

1. Arbitrary Incidence

Consider an infinitely long, perfectly conducting cylinder of circular cross-section with radius a . Let the axis of this cylinder coincide with the Z-axis of a reference coordinate system. We assume that the cylinder has a longitudinal slot, running its entire length, parallel to the axis. The angle this slot subtends at the axis is denoted by ϕ_0 . We shall assume also that the X-axis of the reference rectangular coordinate system lies halfway between the slot edges. Then the XZ-plane bisects the slot. Let us further assume that a linearly polarized, monochromatic, plane electromagnetic wave propagating in the arbitrary direction $\vec{n}(\theta_{inc}, \phi_{inc})$ is irradiating the slotted cylinder. The angle θ_{inc} is the angle between the unit vector \vec{n} and the cylinder axis and, the angle ϕ_{inc} is that between \vec{n} and the XZ-plane. If the wavelength of the incident radiation is λ we have for the incident fields

$$1a) \quad \vec{E}_{inc}(r) = \vec{e}E_0 e^{-ik\vec{n}\cdot\vec{r}}$$

$$1b) \quad \vec{H}_{inc}(r) = \vec{h}H_0 e^{-ik\vec{n}\cdot\vec{r}}$$

where the wave vector for the incident radiation is given by

$$2) \quad \vec{k} \equiv k\vec{n}$$

and

$$3) \quad k \equiv 2\pi/\lambda$$

Also the vectors \vec{e} and \vec{h} are respectively unit vectors in the directions of the incident electric and magnetic fields. We have assumed time dependence of the form $e^{-i\omega t}$ and shall suppress explicit appearance of this harmonic exponential throughout this paper. We show in figure 1 the corresponding geometry of the slotted cylinder and the incident radiation. The angle, p , between the incident electric field and the line of intersection of the XY plane and the plane of the wave front with unit normal vector \vec{n} is called the polarization angle. By allowing this angle, p , to vary from 0 to 2π we can obtain any polarization of the incident field propagated in the direction of \vec{n} . In figure 1 we illustrate the geometry for the case of arbitrary incidence. If we consider the dependence on the transverse coordinates we can write the expansion given by Stratton¹³

$$4) e^{-ik\rho \sin \theta_{inc} \cos(\phi - \phi_{inc})} = \sum_{m=-\infty}^{\infty} (-1)^m e^{im(\phi - \phi_{inc})} J_m(k\rho \sin \theta_{inc})$$

In circular cylindrical coordinates we can then write for the components of the incident fields parallel to the Z-axis

$$5) E_z^i = E_0 \sin \theta_{inc} \sin p e^{-ikz \cos \theta_{inc}} \sum_{m=-\infty}^{\infty} (-1)^m e^{im(\phi - \phi_{inc})} J_m(k\rho \sin \theta_{inc})$$

13. J. Stratton, "Electromagnetic Theory," Sect. 6.10, McGraw-Hill Book Co. New York, N.Y. 1941.

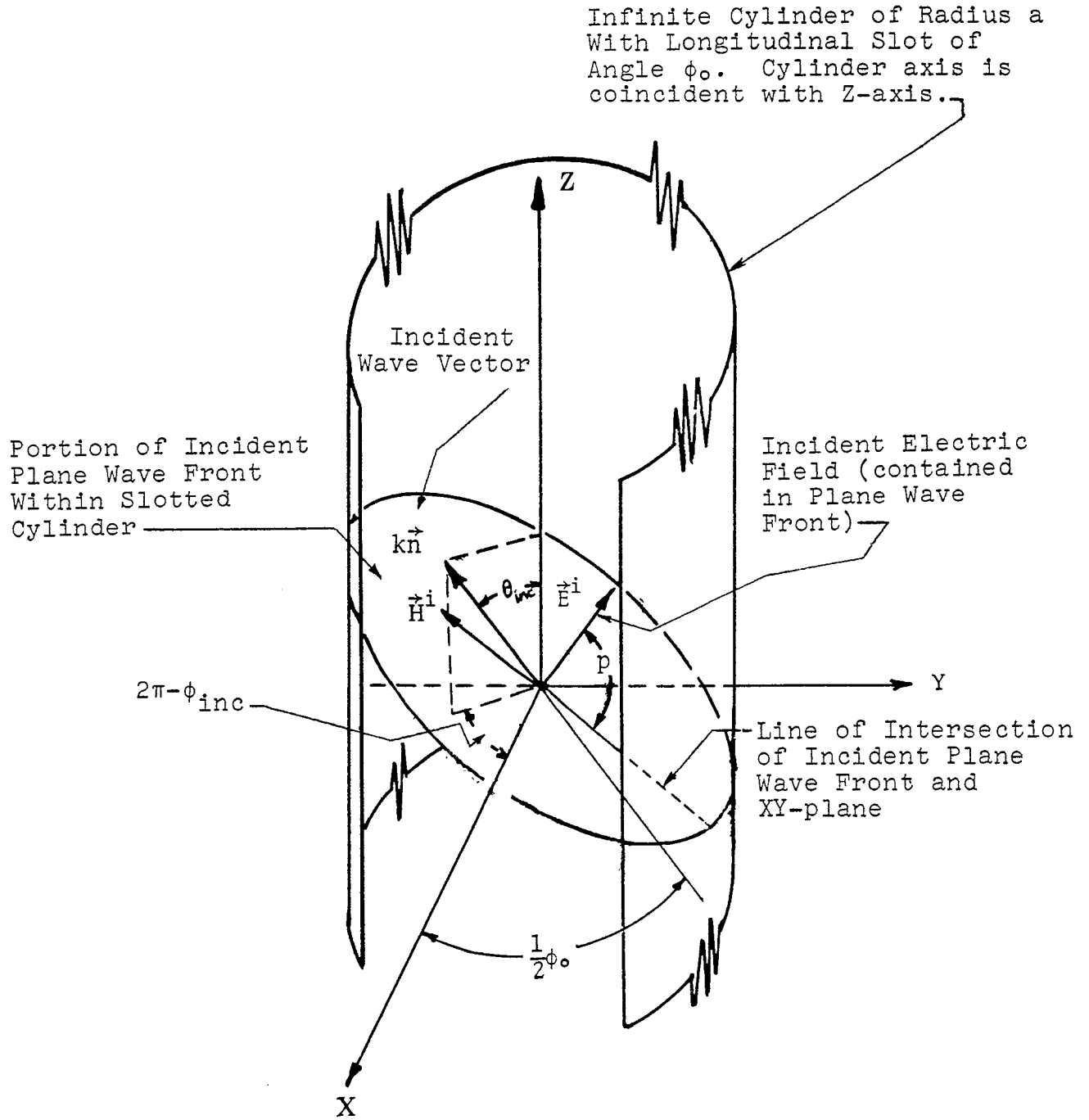


Figure 1. Geometry of Arbitrary Incident Linearly Polarized Plane Wave Irradiating Longitudinally Slotted Circular Cylinder

$$6) H_Z^i = H_0 \sin\theta_{inc} \cos\phi e^{-ikz} \cos\theta_{inc} \sum_{m=-\infty}^{\infty} (-i)^m e^{im(\phi-\phi_{inc})} J_m(k\rho \sin\theta_{inc})$$

The remaining incident field components may then be found using eqs (5) and (6) and the Maxwell equations. As a result of scattering of the incident radiation by the slotted cylinder we obtain outside the cylinder the total longitudinal fields

$$7) E_Z^{(1)}(r) = E_Z^i(r) + E_Z^s(1) \quad \rho > a$$

$$8) H_Z^{(1)}(r) = H_Z^i(r) + H_Z^s(1) \quad \rho > a$$

where we have used the superscript (1) to denote the region exterior to the slotted cylinder. Also E_Z^s and H_Z^s are the scattered field contributions. Similarly interior to the slotted cylinder we have the total longitudinal fields

$$9) E_Z^{(2)}(r) = E_Z^i(r) + E_Z^s(2)(r) \quad \rho < a$$

$$10) H_Z^{(2)}(r) = H_Z^i(r) + H_Z^s(2)(r) \quad \rho < a$$

where the superscript (2) has been appended to denote the region inside the slotted cylinder. Now the scattered fields must vary with the coordinate z in the same manner as the incident field. They must be periodic in ϕ with period 2π and we can therefore

expand them in Fourier series as follows

$$11) \quad E_z^S(r) = E_0 e^{-ikz \cos \theta_{inc}} \sum_{m=-\infty}^{\infty} E_{zm}^S(\rho) e^{im(\phi - \phi_{inc})}$$

$$12) \quad H_z^S(r) = H_0 e^{-ikz \cos \theta_{inc}} \sum_{m=-\infty}^{\infty} H_{zm}^S(\rho) e^{im(\phi - \phi_{inc})}$$

The fields in (11) and (12) must also satisfy the Maxwell equations. Similar expansions hold for the remaining field components. Inside the cylinder the fields are non-singular hence we can readily write

$$13) \quad E_{zm}^{S(2)}(\rho) = A_m^{(2)} \sin \theta_{inc} \sin p \frac{J_m(k\rho \sin \theta_{inc})}{J_m(ka \sin \theta_{inc})}$$

$$14) \quad H_{zm}^{S(2)}(\rho) = B_m^{(2)} \sin \theta_{inc} \cos p \frac{J_m(k\rho \sin \theta_{inc})}{J'_n(ka \sin \theta_{inc})}$$

where the $A_m^{(2)}$ and $B_m^{(2)}$ are expansion coefficients that still must be determined. In the region exterior to the slotted cylinder the fields must have Fourier radial parts of the same form as in eqs (13) and (14). Also we must have an outgoing cylindrical scattered wave as $\rho \rightarrow \infty$. Then we have

$$15) \quad E_{zm}^{s(1)}(\rho) = A_m^{(1)} \sin \theta_{inc} \sin p \frac{H_m^{(1)}(k\rho \sin \theta_{inc})}{H_m^{(1)}(ka \sin \theta_{inc})}$$

$$16) \quad H_{zm}^{s(1)}(\rho) = B_m^{(1)} \sin \theta_{inc} \cos p \frac{H_m^{(1)}(k\rho \sin \theta_{inc})}{H_m^{(1)}(ka \sin \theta_{inc})}$$

where again the $A_m^{(1)}$ and $B_m^{(1)}$ are expansion coefficients that have to be determined. The expansion coefficients must be determined from the boundary conditions at the $\rho=a$ cylinder. Now in the slot we must have the same longitudinal component of field whether we approach the slot from the inside or from the outside. Thus

$$17) \quad E_z^{s(2)}(a, \phi) = E_z^{s(1)}(a, \phi)$$

$$18) \quad H_z^{s(2)}(a, \phi) = H_z^{s(2)}(a, \phi)$$

for all values of ϕ in the slot. Consequently we have

$$19) \quad A_m^{(2)} = A_m^{(1)}$$

$$20) \quad B_m^{(2)} = B_m^{(1)}$$

for all values of m . We shall simply drop the superscripts and henceforth merely write the expansion coefficients as A_m and B_m .

On the conductor we must have the radial component of magnetic field vanishing. This is also true for the longitudinal component of the gradient of the azimuthal component of electric field. We then have at $\rho=a$ using eqs (9) and (13) and the Maxwell equations for $\vec{\nabla} \times \vec{E}$,

$$21) \sum_{m=-\infty}^{\infty} m \left[A_m + (-i)^m J_m(ka \sin \theta_{inc}) \right] e^{im(\phi - \phi_{inc})} = 0$$

$$1/2\phi_0 < \phi < -1/2\phi_0$$

To facilitate the determination of the additional relations generated by the boundary conditions at the slot or on the conductor we shall merely enumerate the explicit forms for the remaining field components. Their derivation is somewhat tedious and the details are omitted. For the incident transverse electric and magnetic fields we have

$$22) H_{\phi}^i(r) = H_0 e^{-ikz \cos \theta_{inc}} \frac{\cos \theta_{inc} \cos p}{k\rho} \sum_{m=-\infty}^{\infty} (-i)^m e^{im(\phi - \phi_{inc})} \cdot$$

$$m J_m(k\rho \sin \theta_{inc}) + E_0 e^{-ikz \cos \theta_{inc}} \frac{ik}{\omega\mu} \sin p \sum_{m=-\infty}^{\infty} (-i)^m e^{im(\phi - \phi_{inc})} \cdot$$

$$J_m'(k\rho \sin \theta_{inc}),$$

$$23) H_{\rho}^i(r) = -H_o e^{-ikz \cos \theta_{inc}} (\cos \theta_{inc} \cos p) \sum_{m=-\infty}^{\infty} (-i)^m e^{im(\phi - \phi_{inc})} \cdot$$

$$J_m'(k\rho \sin \theta_{inc}) + E_o e^{-ikz \cos \theta_{inc}} \frac{1}{\rho \omega \mu} \frac{\sin p}{\sin \theta_{inc}} \sum_{m=-\infty}^{\infty} (-i)^m e^{im(\phi - \phi_{inc})} \cdot$$

$$m J_m(k\rho \sin \theta_{inc}),$$

$$24) E_{\rho}^i(r) = -E_o e^{-ikz \cos \theta_{inc}} \cos \theta_{inc} \sin p \sum_{m=-\infty}^{\infty} (-i)^m e^{im(\phi - \phi_{inc})} \cdot$$

$$J_m'(k\rho \sin \theta_{inc}) - H_o e^{-ikz \cos \theta_{inc}} \frac{1}{\rho \omega \epsilon} \frac{\cos p}{\sin \theta_{inc}} \sum_{m=-\infty}^{\infty} (-i)^m e^{im(\phi - \phi_{inc})} \cdot$$

$$m J_m(k\rho \sin \theta_{inc}),$$

$$25) E_{\phi}^i(r) = E_o e^{-ikz \cos \theta_{inc}} \frac{\cot \theta_{inc}}{k\rho} \sin p \sum_{m=-\infty}^{\infty} (-i)^m e^{im(\phi - \phi_{inc})} \cdot$$

$$J_m(k\rho \sin \theta_{inc}) - H_o e^{-ikz \cos \theta_{inc}} \frac{ik \cos p}{\omega \epsilon} \sum_{m=-\infty}^{\infty} (-i)^m e^{im(\phi - \phi_{inc})} \cdot$$

$$J_m'(k\rho \sin \theta_{inc}).$$

The transverse components of the scattered fields inside and outside the slotted cylinder of radius a are

$$26) E_{\phi}^{s(j)}(\vec{r}) = E_o e^{-ikz \cos \theta_{inc}} \frac{\cot \theta_{inc} \sin p}{k\rho} \sum_{m=-\infty}^{\infty} A_m e^{im(\phi - \phi_{inc})} \cdot$$

$$\frac{Z_m^{(j)}(k\rho \sin \theta_{inc})}{Z_m^{(j)}(k \sin \theta_{inc})} - H_o e^{-ikz \cos \theta_{inc}} \frac{ik \cos \rho}{\omega \epsilon} \sum_{m=-\infty}^{\infty} B_m e^{im(\phi - \phi_{inc})} \cdot$$

$$\frac{Z_m^{(j)'}(k\rho \sin \theta_{inc})}{Z_m^{(j)'}(k \sin \theta_{inc})} ,$$

$$27) E_{\rho}^{s(j)}(\vec{r}) = -iE_o e^{-ikz \cos \theta_{inc}} \cos \theta_{inc} \sin p \sum_{m=-\infty}^{\infty} A_m e^{im(\phi - \phi_{inc})} \cdot$$

$$\frac{Z_m^{(j)'}(k\rho \sin \theta_{inc})}{Z_m^{(j)}(k \sin \theta_{inc})} - \frac{H_o e^{-ikz \cos \theta_{inc}} \cos p}{\omega \epsilon \sin \theta_{inc}} \sum_{m=-\infty}^{\infty} B_m e^{im(\phi - \phi_{inc})} \cdot$$

$$\frac{Z_m^{(j)}(k\rho \sin \theta_{inc})}{Z_m^{(j)'}(k \sin \theta_{inc})} ,$$

$$28) H_{\phi}^{s(j)}(\vec{r}) = H_o e^{-ikz \cos \theta_{inc}} \frac{\cot \theta_{inc} \cos p}{k\rho} \sum_{m=-\infty}^{\infty} B_m e^{im(\phi - \phi_{inc})} \cdot$$

$$\frac{Z_m^{(j)}(k\rho \sin \theta_{inc})}{Z_m^{(j)'}(k \sin \theta_{inc})} + iE_o e^{-ikz \cos \theta_{inc}} \frac{k \sin p}{\omega \mu} \sum_{m=-\infty}^{\infty} A_m e^{im(\phi - \phi_{inc})} \cdot$$

$$\frac{Z_m^{(j)}(k\rho \sin\theta_{inc})}{Z_m^{(j)}(ka \sin\theta_{inc})},$$

$$29) H_p^{s(j)}(\vec{r}) = -iH_0 e^{-ikz \cos\theta_{inc}} \cos\theta_{inc} \cos p \sum_{m=-\infty}^{\infty} B_m e^{im(\phi - \phi_{inc})}.$$

$$\frac{Z_m^{(j)}(k\rho \sin\theta_{inc})}{Z_m^{(j)}(ka \sin\theta_{inc})} + E_0 e^{-ikz \cos\theta_{inc}} \frac{\sin p}{\sin\theta_{inc}} \frac{1}{\rho\omega\mu} \sum_{m=-\infty}^{\infty} A_m e^{im(\phi - \phi_{inc})}.$$

$$\frac{Z_m^{(j)}(k\rho \sin\theta_{inc})}{Z_m^{(j)}(ka \sin\theta_{inc})}.$$

In eqs (26) through (29) we have the interior components if $j=2$ and the exterior components if $j=1$. For $j=2$ one has to replace $Z_m(\)$ by the Bessel function $J_m(\)$, whereas for $j=1$ the function $Z_m(\)$ must be replaced by the Hankel function $H_m^{(1)}(\)$.

Now the radial component of the magnetic field is continuous across the cylindrical surface, at $\rho=a$, over the slot. Then we have

$$\frac{\partial E_\rho^{s(2)}}{\partial z} - \frac{\partial E_z^{s(2)}}{\partial \rho} = \frac{\partial E_\rho^{s(1)}}{\partial z} - \frac{\partial E_z^{s(1)}}{\partial \rho}$$

After some manipulation, substitution from eqs (13), (14) and their equivalents outside the cylinder, and eq (27) for $j=1$ and $j=2$ yields the additional relation for the expansion coefficients A_m

$$30) \quad \sum_{m=-\infty}^{\infty} \frac{A_m e^{im(\phi-\phi_{inc})}}{J_m(k \sin \theta_{inc}) H_m^{(1)}(k \sin \theta_{inc})} = 0$$

To obtain eq (30) we had to make use of the Wronskian for $J_m(X)$ and $H_m^{(1)}(X)$. In much the same manner we obtain another relation for the expansion coefficients A_m by applying boundary conditions on the slot.

$$31) \quad \sum_{m=-\infty}^{\infty} (-1)^m \left[A_m + (-i)^m J_m'(k \sin \theta_{inc}) \right] e^{-im\phi_{inc}} = 0$$

The details of the derivation of eq (31) are straightforward and we have omitted them here. Similarly we can obtain three relations that the expansion coefficients B_m satisfy. These are

$$32) \quad \sum_{m=-\infty}^{\infty} \left[B_m + (-i)^m J_m'(k \sin \theta_{inc}) \right] e^{im(\phi-\phi_{inc})} = 0$$

$$33) \quad \sum_{m=-\infty}^{\infty} m B_m \frac{e^{im(\phi-\phi_{inc})}}{J_m(k \sin \theta_{inc}) H_m^{(1)'}(k \sin \theta_{inc})} = 0$$

$$34) \quad \sum_{m=-\infty}^{\infty} \frac{B_m e^{-im\phi_{inc}}}{J_m'(k \sin \theta_{inc}) H_m^{(1)'}(k \sin \theta_{inc})} = 0$$

Eq (32) is obtained from the boundary conditions applied at the metal on the inside. Eq (33) and (34) are obtained at the slot by applying boundary conditions. Again we have omitted the details of the derivation.

Let us focus our attention on eqs (21), (30) and (31) which represent simultaneous relations that the infinite set of expansion coefficients A_m must satisfy. It is more productive to introduce new forms for the unknown quantities. Thus we define

$$35) \quad X_m \equiv m \left[A_m + (-i)^m J_m(k a \sin \theta_{inc}) \right] e^{-im\phi_{inc}} \quad \text{for } m \neq 0$$

$$36) \quad X_0 \equiv \left[A_0 + J_0(k a \sin \theta_{inc}) \right]$$

For additional convenience we also introduce the quantity

$$37) \quad g_m \equiv 1 - \frac{1}{\pi i |m| J_m(k a \sin \theta_{inc}) H_m^{(1)}(k a \sin \theta_{inc})}$$

It should be noted that g_m goes to zero like $1/|m|^2$ as $m \rightarrow \infty$.¹⁴ We can then write, after some rearranging, in place of eqs (21), (30) and (31)

$$38) \quad \sum_{m=-\infty}^{\infty} X_m e^{im\phi} = 0 \quad \text{for } \frac{1}{2}\phi_0 < |\phi| \leq \pi$$

14. A. Erdélyi, Ed. "California Institute of Technology, Bateman Manuscript Project. Higher Transcendental Functions Vol. II," eqs. (13) and (14) p. 87, McGraw-Hill Book Co. Inc. New York NY 1953.

$$\begin{aligned}
 39) \quad \sum_{m=-\infty}^{\infty}{}' X_m \frac{|m|}{m} e^{im\phi} &= \frac{i}{\pi} \frac{X_0}{J_0(k a \sin \theta_{inc}) H_0^{(1)}(k a \sin \theta_{inc})} + \\
 &+ \sum_{m=-\infty}^{\infty}{}' X_m \frac{|m|}{m} g_m e^{im\phi} - \frac{i}{\pi} \sum_{m=-\infty}^{\infty}{}' \frac{(-i)^m e^{-im\phi_{inc}}}{H_m^{(1)}(k a \sin \theta_{inc})} e^{im\phi} \\
 &\text{for } |\phi| < \frac{1}{2}\phi_0.
 \end{aligned}$$

$$40) \quad \sum_{m=-\infty}^{\infty}{}' (-1)^m \frac{X_m}{m} = -X_0 \quad \text{for } |\phi| < \frac{1}{2}\phi_0.$$

In eqs (38), (39) and (40) the prime on the summation sign indicates that the summation index does not take on the value zero. Agranovich et.al.¹⁵ have shown that eqs (38), (39) and (40) are in standard form for application of the Riemann-Hilbert method of solution for the set of unknowns X_0 and X_m .

By this procedure we can cast eqs (38), (39) and (40) in the following form i.e. an infinite system of linear, inhomogeneous, simultaneous equations.

15. Z. S. Agranovich, V. A. Marchenko and V. P. Shestopalov, "Diffraction of Electromagnetic Waves By Plane Metallic Gratings," Zh. tekn. Fiz. 32, No. 4, 381 (1962).

$$41) \quad X_n = \frac{i}{\pi} \frac{A_o V_n^o(u)}{J_o(k \sin \theta_{inc}) H_o^{(1)}(k \sin \theta_{inc})} + \sum_{m=-\infty}^{\infty} X_m \frac{|m|}{m} g_m V_n^m(u) -$$

$$-\frac{i}{\pi} \sum_{m=-\infty}^{\infty} (-i)^m \frac{e^{-im\phi_{inc}} V_n^m(u)}{H_m^{(1)}(k \sin \theta_{inc})} + 2X_{-1} R_n(u),$$

$$42) \quad 0 = \frac{i}{\pi} \frac{A_o V_o^o(u)}{J_o(k \sin \theta_{inc}) H_o^{(1)}(k \sin \theta_{inc})} + \sum_{m=-\infty}^{\infty} X_m \frac{|m|}{m} g_m V_o^m(u) -$$

$$-\frac{i}{\pi} \sum_{m=-\infty}^{\infty} (-i)^m \frac{e^{-im\phi_{inc}} V_o^m(u)}{H_m^{(1)}(k \sin \theta_{inc})} + 2X_{-1} R_o(u),$$

$$43) \quad -A_o = \frac{i}{\pi} \frac{A_o V_\sigma^o(u)}{J_o(k \sin \theta_{inc}) H_o^{(1)}(k \sin \theta_{inc})} + \sum_{m=-\infty}^{\infty} X_m \frac{|m|}{m} g_m V_\sigma^m(u) -$$

$$-\frac{i}{\pi} \sum_{m=-\infty}^{\infty} (-i)^m \frac{e^{-im\phi_{inc}} V_\sigma^m(u)}{H_m^{(1)}(k \sin \theta_{inc})} + 2X_{-1} R_\sigma(u),$$

where the coefficients introduced into these equations are, for future reference, the following

$$44) \quad R_n(u) \equiv \frac{1}{2\pi} \int_{-\frac{1}{2}\phi_0}^{\frac{1}{2}\phi_0} d\phi \frac{e^{-in\phi}}{\sqrt{(e^{i\phi} - e^{i\phi_0/2})(e^{i\phi} - e^{-i\phi_0/2})}}$$

$$= \frac{1}{2} P_{-n-1}(u) = \frac{1}{2} P_n(u)$$

$$45) \quad V_n^m(u) = \frac{(n+1)}{2(n-m)} \left[P_n(u)P_{m+1}(u) - P_{n+1}(u)P_m(u) \right] \quad \text{for } n \neq m$$

$$46) \quad R_\sigma(u) \equiv -\frac{1}{2} \ln\left(\frac{1+u}{2}\right)$$

$$47) \quad V_\sigma^m(u) \left\{ \begin{array}{l} \equiv -\frac{1}{2} \left[P_{m+1}(u) - 2uP_m(u) + P_{m-1}(u) \right] \ln\left(\frac{1+u}{2}\right) + \\ + \frac{1}{2m} \left[P_m(u) - P_{m-1}(u) \right] \quad \text{for } m \geq 1 \\ \equiv \left(\frac{1+u}{2}\right) \ln\left(\frac{1+u}{2}\right) \quad \text{for } m=0 \\ \equiv \left(\frac{u-1}{2}\right) \ln\left(\frac{1+u}{2}\right) + \left(\frac{u-1}{2}\right) \quad \text{for } m=-1 \\ \equiv -\frac{1}{2} \left[P_{-m}(u) - 2uP_{-m-1}(u) + P_{-m-2}(u) \right] \ln\left(\frac{1+u}{2}\right) \\ -\frac{1}{2m} \left[P_{-m}(u) - P_{-m-1}(u) \right] \quad \text{for } m < -1 \end{array} \right.$$

In eqs (44) through (47) the functions $P_n(u)$ are Legendre polynomials. and the variable we have been using is

$$48) \quad u \equiv \cos\left(\frac{1}{2}\phi_0\right)$$

For the system of equations (32), (33) and (34) which determine the remaining unknown expansion coefficients, B_m , a similar transformation can be effected by introducing new definitions. Thus if we define

$$49) \quad Y_m \equiv \frac{(-1)^m B_m e^{-im\phi_{inc}}}{J_m'(k a \sin\theta_{inc}) H_m^{(1)'}(k a \sin\theta_{inc})}$$

and

$$50) \quad G_m \equiv 1 - \frac{i\pi}{|m|} (k a \sin\theta_{inc})^2 J_m'(k a \sin\theta_{inc}) H_m^{(1)'}(k a \sin\theta_{inc})$$

where $G_m \rightarrow 0$ like $1/|m|^2$ as $m \rightarrow \infty$ we can obtain another infinite system of linear, inhomogeneous, simultaneous equations. These are as follows:

with the additional definition

$$51) \quad Y_0 = B_0 / J_0'(k a \sin\theta_{inc}) H_0^{(1)'}(k a \sin\theta_{inc})$$

$$\begin{aligned}
52) \quad Y_n &= i\pi Y_o (k \sin \theta_{inc})^2 J_o'(k \sin \theta_{inc}) H_o^{(1)'}(k \sin \theta_{inc}) V_n^o(-u) + \\
&+ \sum_{m=-\infty}^{\infty} Y_m \frac{|m|}{m} G_m V_n^m(-u) - i\pi (k \sin \theta_{inc})^2 \sum_{m=-\infty}^{\infty} (-i)^m e^{im\phi_{inc}} \cdot \\
&\cdot J_m'(k \sin \theta_{inc}) V_n^m(-u) + 2Y_{-1} R_n(-u),
\end{aligned}$$

$$\begin{aligned}
53) \quad 0 &= -i\pi Y_o (k \sin \theta_{inc})^2 J_o'(k \sin \theta_{inc}) H_o'(k \sin \theta_{inc}) V_o^o(-u) + \\
&+ \sum_{m=-\infty}^{\infty} Y_m \frac{|m|}{m} G_m V_o^m(-u) - i\pi (k \sin \theta_{inc})^2 \sum_{m=-\infty}^{\infty} (-i)^m e^{im\phi_{inc}} \cdot \\
&\cdot J_m'(k \sin \theta_{inc}) V_o^m(-u) + 2Y_{-1} R_o(-u),
\end{aligned}$$

$$\begin{aligned}
54) \quad -Y_o &= -i\pi Y_o (k \sin \theta_{inc})^2 J_o'(k \sin \theta_{inc}) H_o^{(1)'}(k \sin \theta_{inc}) V_o^o(-u) + \\
&+ \sum_{m=-\infty}^{\infty} Y_m \frac{|m|}{m} G_m V_o^m(-u) - i\pi (k \sin \theta_{inc})^2 \sum_{m=-\infty}^{\infty} (-i)^m e^{im\phi_{inc}} \cdot \\
&\cdot J_m'(k \sin \theta_{inc}) V_o^m(-u) + 2Y_{-1} R_o(-u),
\end{aligned}$$

where the coefficients $R_n(-u)$, $V_n^m(-u)$, $R_o(-u)$, $V_o^m(-u)$ are defined in equations (44) through (47). Now, however, we have the argument $-u \equiv -\cos \frac{1}{2} \phi_o$ in the expressions.

For arbitrary values of the cylinder parameters and for an arbitrary incident plane wave solution of the two systems embodied in eqs (38), (39) and (40) and also eqs (52), (53) and (54) will yield complete knowledge of the interior and exterior fields.

2. E-polarization and Arbitrary Incidence in Plane of Symmetry Through the Slot.

In their study of the narrow slotted circular cylinder Morse and Feshbach⁶ showed that resonance phenomena were not affected by the choice of ϕ_{inc} for the incident plane wave. They did not investigate the effect on the resonances of the choice of θ_{inc} . Koshparënok and Shestopalov did look into this property and we shall proceed to expound on this subject now.

We shall assume $\phi_{inc} = \pi$ and $p = \pi/2$. This results in setting all z-components of the magnetic field identically to zero everywhere. This situation we refer to, in the more general sense, as E-polarization. Thus we find that for an E-polarized incident wave the scattered fields are determined solely by the expansion coefficients A_m . Note that we are now considering the plane wave to be incident on the slotted cylinder toward the slot. We first note that from eq (35) we have for $\phi_{inc} = \pi$

$$55) \quad \frac{X_m}{m} = (-1)^m \left[A_m + (-i)^m J_m(k a \sin \theta_{inc}) \right]$$

6. P. M. Morse and H. Feshbach, Ibid.

Then since $J_{-m}(\alpha) = (-1)^m J_m(\alpha)$ we obtain upon replacing m by $-m$

$$-\frac{X_{-m}}{m} = (-1)^m \left[A_{-m} + (-i)^m J_m(k a \sin \theta_{inc}) \right]$$

Then we have

$$56) \quad X_{-m} = -X_m$$

$$57) \quad A_{-m} = A_m$$

To tidy up the appearance of some relations we introduce some new notation,

$$58) \quad \alpha_m \equiv \frac{X_m}{m}, \quad a_0 \equiv X_0$$

Then the total field components interior to the slotted cylinder may be rewritten as

$$59) \quad E_z^{(2)}(\vec{r}) = E_0 \sin \theta_{inc} e^{-ikz \cos \theta_{inc}} \sum_{m=0}^{\infty} \epsilon_m \alpha_m \frac{J_m(k \rho \sin \theta_{inc})}{J_m(k a \sin \theta_{inc})} \cos m\phi$$

$$60) \quad E_\phi^{(2)}(\vec{r}) = 2iE_0 \frac{\cot \theta_{inc}}{k\rho} e^{-ikz \cos \theta_{inc}} \sum_{m=1}^{\infty} m \alpha_m \frac{J_m(k \rho \sin \theta_{inc})}{J_m(k a \sin \theta_{inc})} \sin m\phi$$

$$61) \quad E_\rho^{(2)}(\vec{r}) = iE_0 \cos \theta_{inc} e^{-ikz \cos \theta_{inc}} \sum_{m=0}^{\infty} \epsilon_m \alpha_m \frac{J'_m(k \rho \sin \theta_{inc})}{J_m(k a \sin \theta_{inc})} \cos m\phi$$

$$62) \quad H_z^{(2)}(\vec{r}) \equiv 0$$

$$63) \quad H_\phi^{(2)}(\vec{r}) = iH_o e^{-ikz \cos \theta_{inc}} \sum_{m=0}^{\infty} \epsilon_m \alpha_m \frac{J'_m(k\rho \sin \theta_{inc})}{J'_m(k a \sin \theta_{inc})} \cos m\phi$$

$$64) \quad H_\rho^{(2)}(\vec{r}) = \frac{2iH_o}{k\rho \sin \theta_{inc}} e^{-ikz \cos \theta_{inc}} \sum_{m=1}^{\infty} m \alpha_m \frac{J_m(k\rho \sin \theta_{inc})}{J_m(k a \sin \theta_{inc})} \sin m\phi$$

where we have

$$65) \quad \epsilon_m = \begin{cases} 1 & \text{if } m=0 \\ 2 & \text{if } m \neq 0 \end{cases}$$

and we have also used the relation

$$66) \quad H_o = \frac{k}{\omega \mu} E_o = \sqrt{\frac{\epsilon}{\mu}} E_o = Z_o^{-1} E_o$$

where Z_o is the free space impedance. Upon examination of eq (37) we observe that

$$g_{-m} = g_m$$

then we can write the following compact set of relations in place of eqs (41), (42) and (43)

$$67) \quad X_n = \sum_{m=0}^{\infty} \alpha_{nm} X_m + \beta_n$$

where it can be shown

$$68) \quad \alpha_{nm} \equiv \frac{g_m}{2} \sum_{j=0}^m \mu_{m-j}(u) \left[P_{j-n}(u) - P_{j+n}(u) \right] \quad \text{for } n, m \neq 0$$

$$69) \quad \alpha_{no} \equiv \frac{i}{\pi} \frac{V_{n-1}^{-1}(u)}{J_0(k \sin \theta_{inc}) H_0^{(1)}(k \sin \theta_{inc})} \quad \text{for } n \neq 0$$

$$70) \quad \alpha_{oo} \equiv -\frac{i}{\pi} \frac{\ln \left[\frac{1+u}{2} \right]}{J_0(k \sin \theta_{inc}) H_0^{(1)}(k \sin \theta_{inc})}$$

$$71) \quad \alpha_{om} \equiv -\frac{\epsilon_m}{m} \left[P_m(u) - P_{m-1}(u) \right] \quad m \neq 0$$

We have in the above introduced the notation

$$72) \quad \mu_j(u) \equiv \begin{cases} 1 & \text{for } j=0 \\ -u & \text{for } j=1 \\ P_j(u) - 2uP_{j-1}(u) + P_{j-2}(u) & \text{for } j \geq 2 \end{cases}$$

Of course $P_j(u)$ is still a Legendre polynomial of argument $u = \cos \frac{1}{2} \phi_0$. Furthermore the β_n in eq (67) are defined as follows

$$73) \quad \beta_n \equiv -\frac{i}{\pi} \sum_{m=0}^{\infty} (-i)^m \frac{1}{H_m^{(1)}(k \sin \theta_{inc})} \sum_{j=0}^m \mu_{m-j}(u) \left[P_{j-n}(u) - P_{j+n}(u) \right]$$

$$74) \quad \beta_o = \frac{i}{\pi} \frac{\ln \left[\frac{1+u}{2} \right]}{H_0^{(1)}(k \sin \theta_{inc})} + \frac{i}{2\pi} \sum_{m=1}^{\infty} (-i)^m \frac{\epsilon_m}{m} \frac{\left[P_m(u) - P_{m-1}(u) \right]}{H_m^{(1)}(k \sin \theta_{inc})}$$

Although we have set up the general problem for arbitrary incidence in the preceding subsection and reduced it to the case of $\phi_{inc} = \pi$

and $p=\pi/2$ in this subsection we will nevertheless not proceed to process the equations further toward the general solution in even this restricted situation. This is left as the subject of a future paper. What we shall however consider is interior electric fields in the significant case in which the longitudinal slot is very narrow. We shall focus our attention for this situation on two cases in succession. The first is when the values of $kasin\theta_{inc}$ are not too close to the roots of the zero order ordinary Bessel function, J_0 . The second case we consider is when the values of $kasin\theta_{inc}$ are in fact close to the roots of J_0 . Let us proceed to these cases. We begin with the observation that for $kasin\theta_{inc} \sim v_{sn}$, where the v_{sn} are the roots of the Bessel function $J_s(kasin\theta_{inc})$, certain of the coefficients α_{nm} in eq (67) may blow up without bounds. For the purposes of this paper we consider the specific case where:

$$kasin\theta_{inc} \rightarrow v_{on} \text{ and } J_0(kasin\theta_{inc}) \rightarrow 0.$$

Now the coefficients α_{no} do not become infinite in all instances. This is due to the fact that their numerators may go to zero at least as fast as their denominators. Consider then α_{oo} as given in eq (70). We have to examine only

$$\ln\left[\frac{1}{2}(1+u)\right] / J_0(kasin\theta_{inc})$$

For a narrow slot

$$75) \quad \ln \left[\frac{1}{2}(1+u) \right] = \ln \frac{1}{2} (1 + \cos \frac{1}{2} \phi_0) = \ln \cos^2 \left(\frac{1}{4} \phi_0 \right) \approx - \phi_0^2 / 16$$

which for a 10° slot is about 0.002 in value. Let us write $k \sin \theta_{inc} = v_{on} + \delta$. Then we have for small δ

$$76) \quad J_0(k \sin \theta_{inc}) = J_0(v_{on} + \delta) \approx \delta J_1(v_{on})$$

In turn we have

$$77) \quad \frac{\ln \frac{1}{2}(1+u)}{J_0(k \sin \theta_{inc})} \approx \frac{\phi_0^2}{16 \delta J_1(v_{on})}$$

In the same way we can investigate α_{no} from eq (69) for $k \sin \theta_{inc}$ values near v_{on} . We merely need to consider $V_{n-1}^{-1}(u) / J_0(k \sin \theta_{inc})$. It is an easy matter to show from the definition of the Legendre polynomial that¹⁶

$$78) \quad P_{n-1}(u) - P_n(u) = \frac{(1-u)}{n} \sum_{j=0}^{n-1} (2j+1) P_j(u)$$

It can be shown readily enough that a good estimate for the Legendre polynomials leads to

$$V_{n-1}^{-1}(u) = \frac{(1-u)}{2n} \sum_{j=0}^{n-1} (2j+1) P_j(u) \leq n \phi_0^2 / 16$$

16. I. S. Gradshteyn and I. W. Ryzhik, "Tables of Integrals Series and Products," Sect. 8.91, Academic Press, N.Y., N.Y., 1965.

and consequently

$$79) \frac{V_{n-1}^{-1}(u)}{J_0(k a \sin \theta_{inc})} \approx \frac{n \phi_0^2}{16 \delta J_1(v_{on})}$$

Near the roots of $J_0(k a \sin \theta_{inc})$ the remaining α_{nm} coefficients are well behaved.

Now let us consider explicitly the case where the longitudinal slot in the conducting cylinder is very narrow and $k a \sin \theta_{inc}$ takes on values that are not too close to the roots of the zero-order Bessel function of the first kind. That is we are considering the situation for which

$$80) \phi_0^2 \ll \delta J_1(v_{on})$$

For this situation all the coefficients α_{mn} decrease rather rapidly and eq (67) can be solved by successive approximation. We can achieve a good qualitative analysis of the fields interior to the narrowly slotted cylinder by constraining ourselves to the following approximation

$$81) X_n \approx \beta_n = -\frac{i}{\pi} \sum_{m=0}^{\infty} \frac{(-i)^m}{H_m^{(1)}(k a \sin \theta_{inc})} \sum_{j=0}^m \mu_{m-j}(u) [P_{j-n}(u) - P_{j+n}(u)]$$

for $n \neq 0$

$$82) \quad X_o \approx \beta_o = \frac{i}{\pi} \frac{\ln\left[\frac{1}{2}(1+u)\right]}{H_o^{(1)}(k \sin \theta_{inc})} + \frac{i}{2\pi} \sum_{m=1}^{\infty} (-1)^m \frac{\epsilon_m}{m} \frac{[P_m(u) - P_{m-1}(u)]}{H_m^{(1)}(k \sin \theta_{inc})}$$

It follows easily enough from eqs (81) and (82) that

$$83) \quad X_n < -\frac{i}{\pi} \sin^2\left(\frac{\phi_o}{4}\right) \sum_{m=0}^{\infty} (-1)^m \frac{\ln(m+1)}{H_m^{(1)}(k \sin \theta_{inc})} \quad \text{for } n \neq 0$$

and

$$84) \quad X_o < \frac{i}{\pi} \sin^2\left(\frac{\phi_o}{4}\right) \sum_{m=0}^{\infty} \epsilon_m (-1)^m \frac{m}{H_m^{(1)}(k \sin \theta_{inc})}$$

The series appearing in eqs (83) and (84) converge nicely and we then have

$$85) \quad X_m < \text{constant} \times \phi_o^2, \quad X_o < \text{constant} \times \phi_o^2$$

where the constants in eq (85) are finite and well behaved. We thus have established analytically what we have seen earlier by numerical calculation^{3,4} namely far from certain values called resonance values when the longitudinal slot in the circular conducting cylinder is very narrow the electric field in the slot is very small. Simultaneously the penetration of the field through the slot into the interior is very strongly inhibited. We can also observe that analytically

3. J. N. Bomhardt and L. F. Libelo, S.E.R.A. V. op.cit.

4. L. F. Libelo, A.G. Henney, J.N. Bomhardt and F.S.Libelo, S.E.R.A.X. op.cit.

as the slot increases in size the aperture field tends to increase. The leakage field inside the slotted cylinder is still very small but does increase with increasing slot angle. We also demonstrated this by numerical means earlier.

We can now emphasize a very interesting characteristic that has emerged from the theoretical manipulations. This is the fact that even for frequencies of the incident field which do not coincide with the circular waveguide frequencies (which for narrow slotted cylinders lie very close to the slotted cylinder resonances) by appropriately choosing the angle of incidence θ_{inc} values of $k a \sin \theta_{inc}$ can be attained such that resonant excitation of the slotted cylinder results. For such choices of the direction of incidence we have $\phi_0^2 \gg \delta J_1(v_{on})$. This situation in fact brings us to the second case we wish to consider. We next proceed to investigate this case in some detail i.e. for $k a \sin \theta_{inc}$ near the roots of the Bessel functions, $J_n(\)$, and the slot in the conducting cylinder is still a narrow one.

When $k a \sin \theta_{inc}$ is close to the value of a root of $J_n(k a \sin \theta_{inc})$ we can have coefficients α_{1j} in eq (47) that are very large compared to unity. In this case the method of successive approximations no longer can be safely relied upon to solve for the expansion coefficients in the series representations of the fields. We shall investigate this case in a different manner. For purposes of convenience and emphasis we rewrite eq (47) as

$$86) \quad X_n = \alpha_{no} X_o + \sum_{m=1}^{\infty} \alpha_{nm} X_m + B_n$$

$$87) \quad X_0 = \alpha_{00} X_0 + \sum_{m=1}^{\infty} \alpha_{0m} X_m + B_0$$

Now we recall that the longitudinal slot in the conducting cylinder is a narrow one. Then all the coefficients α_{nm} for $n, m \neq 0$ are small. Consequently the system of equations with these α_{nm} removed can be solved by successive approximation. Writing the first approximation in the form

$$88) \quad X_n \approx \alpha_{n0} X_0 + \beta_n \quad \text{for } n \neq 0$$

and substituting this into eq (87) we obtain an approximate expression for X_0 .

$$89) \quad X_0 = \left[\sum_{m=1}^{\infty} \alpha_{0m} \beta_m + \beta_0 \right] / \left[1 - \alpha_{00} - \sum_{m=1}^{\infty} \alpha_{0m} \alpha_{m0} \right]$$

If we reexamine eqs (59) through (64), the expressions for the components of the electric and magnetic fields inside the slotted conducting circular cylinder, we find that each non-vanishing one contains the quantities

$$90) \quad a_m \equiv \alpha_m / J_m(k a \sin \theta_{inc})$$

We can evaluate the leading terms in an expansion of a_m in eq (90) in powers of the narrow slot angle ϕ_0 . In doing so we shall drop all terms beyond ϕ_0^2 . This essentially will be an expansion of the

unknowns X_n , and in turn the field components themselves. First consider X . By the definition of β_o in eq (74) and eqs (75) and (78) we have

$$91) \quad \beta_o \approx \left\{ \frac{1}{16\pi H_o^{(1)}(k \sin \theta_{inc})} - \frac{1}{8\pi} \sum_{m=1}^{\infty} \frac{(-1)^m}{m H_m^{(1)}(k \sin \theta_{inc})} \right\} \phi_o^2$$

$$\approx \text{constant} \cdot \phi_o^2$$

Examination of β_n as defined in eq (73) and considering eqs (78) and (72) we note that for $n \neq 0$ the leading term in the β_n expansion will be linear in ϕ_o and the next term will be of order ϕ_o^3 . Thus

$$92) \quad \beta_n \approx \text{constant} \cdot \phi_o$$

By eqs (37) for g_m and (71) for α_{om} and also eqs (69) for α_{no} and (79) we observe that

$$93) \quad \alpha_{om} \alpha_{mo} \approx \text{constant} \cdot \phi_o^4$$

Hence we can drop the summations on $\alpha_{om} \alpha_{mo}$ and on $\alpha_{om} \beta_m$. Next we examine α_{oo} . We found that by eqs (70) and (77) this goes as

$$94) \quad \alpha_{oo} \approx \left\{ - \frac{1}{16\pi J_1(v_{on}) H_o^{(1)}(k \sin \theta_{inc})} \right\} \frac{\phi_o^2}{\delta} \approx \text{constant} \cdot \frac{\phi_o^2}{\delta}$$

Thus to second order in the narrow slot angle ϕ_o we have

$$\alpha_o \equiv X_o \approx \beta_o / (1 - \alpha_{oo})$$

and hence

$$a_0 = \frac{\alpha_0}{J_0(k a \sin \theta_{inc})} \approx \frac{\beta_0}{[J_0(k a \sin \theta_{inc}) - \alpha_{00} J_0(k a \sin \theta_{inc})]}$$

or to second order in the slot angle ϕ_0

$$95) a_0 \approx \frac{i}{u} \left\{ \frac{\ln \left[\frac{1}{2}(1+u) \right]}{H_0^{(1)}(k a \sin \theta_{inc})} + \frac{1}{2} \sum_{m=1}^{\infty} \frac{(-i)^m \epsilon_m}{m} \frac{[P_m(u) - P_{m-1}(u)]}{H_m^{(1)}(k a \sin \theta_{inc})} \right\} /$$

$$\left\{ J_0(k a \sin \theta_{inc}) + \frac{i}{\pi} \frac{\ln \left[\frac{1}{2}(1+u) \right]}{H_0^{(1)}(k a \sin \theta_{inc})} \right\}$$

Note that if $\delta \ll \phi_0^2$ we have

$$96) a_0 \sim \left(\frac{\text{constant} \cdot \phi_0^2}{1 - \text{constant}' \cdot \delta^{-1} \phi_0^2} \right) \frac{1}{\delta J_1(v_{on})} = \frac{\text{constant} \cdot \phi_0^2}{J_1(v_{on}) [\delta - \text{constant}' \cdot \phi_0^2]}$$

$$= \frac{\text{constant}}{J_1(v_{on}) \left(\frac{\delta}{\phi_0^2} - \text{constant}' \right)} \approx \text{constant}$$

Thus as $\delta \rightarrow 0$ and ϕ_0 becomes very small but remains non-zero we find that the quantity a_0 remains finite. This corresponds physically to the infinitely sharp circular waveguide resonance near v_{on} becoming an ever so slightly broadened line with a relatively large but finite amplitude when a very narrow slot is present in the conducting circular cylinder. This is essentially a manifestation

of what we had found for larger slot angles occurring as it should in the limit of narrow slot angles. There is a fundamental difference here though. For the previous analyses for larger slot angles we considered normal, symmetric incidence whereas here for the very narrow slots we are still considering symmetric but not necessarily normal incidence on the slotted cylinder.

We still have to consider the remaining factors

$$a_m = \frac{\alpha_m}{J_m(k a \sin \theta_{inc})} = \frac{X_m}{m J_m(k a \sin \theta_{inc})} \quad \text{for } m \neq 0$$

By eq (88) we have

$$a_m \approx \frac{\alpha_{m0} X_0 + \beta_m}{m J_m(k a \sin \theta_{inc})} = \frac{1}{m J_m(k a \sin \theta_{inc})} \left\{ \frac{a_0 V_{m-1}^{-1}(u)}{H_0^{(1)}(k a \sin \theta_{inc})} + \beta_m \right\}$$

The last relation follows from eq (69) and the definition of a_0 .

Using the definition of β_m in eq (73) we obtain

$$97) \quad a_m = \frac{1}{\pi} \frac{1}{m J_m(k a \sin \theta_{inc})} \left\{ \frac{a_0 V_{m-1}^{-1}(u)}{H_0^{(1)}(k a \sin \theta_{inc})} - \sum_{n=0}^{\infty} \frac{(-i)^n}{H_n^{(1)}(k a \sin \theta_{inc})} \right. \\ \left. \sum_{j=0}^n \mu_{n-j}(u) \cdot [P_{j-m}(u) - P_{j+m}(u)] \right\}$$

Now for small ϕ_0 , a_0 becomes approximately the constant of eq (96), $V_{m-1}^{-1}(u)$ as we indicated just above eq (79) becomes approximately proportional to ϕ_0^2 and the quantity

$$\sum_{j=0}^n u_{n-j}(u) [P_{j-m}(u) - P_{j+m}(u)]$$

expands into a term proportional to ϕ_0 and successive terms of higher order in ϕ_0 . Consequently for all $m > 0$, for narrow slot angles and very small values of δ we have

$$98) \quad \alpha_m \ll \alpha_0$$

We then can write for values of $k a \sin \theta_{inc}$ near the roots of the zero-order Bessel functions that the components of the fields interior to the slot circular conducting cylinder are from eqs (59) through (64)

$$99) \quad E_z^{(2)}(\vec{r}) \approx E_0 a_0 \sin \theta_{inc} e^{ikz \cos \theta_{inc}} J_0(k a \sin \theta_{inc})$$

$$100) \quad E_p^{(2)}(\vec{r}) \approx -i E_0 a_0 \cos \theta_{inc} e^{ikz \cos \theta_{inc}} J_0'(k a \sin \theta_{inc})$$

$$101) \quad E_\phi^{(2)}(\vec{r}) \approx 0$$

$$102) H_z^{(2)}(\vec{r}) = 0$$

$$103) H_\rho^{(2)}(\vec{r}) \approx 0$$

$$104) H_\phi^{(2)}(\vec{r}) \approx iH_0 \alpha_0 e^{-ikz \cos \theta_{inc}} J_0'(k\rho \sin \theta_{inc})$$

We can now draw some conclusions for arbitrary angle of incidence θ_{inc} of an E-polarized plane electromagnetic wave on a circular conducting cylinder with a narrow longitudinal slot. The fields will only weakly penetrate into the cylinder except at certain frequencies and values of the angle θ_{inc} . These frequencies of the incident radiation correspond to those values of $k \sin \theta_{inc}$ which are very close to the roots of the zero order Bessel function $J_0(\cdot)$. At these frequencies interior fields of rather substantial, but finite, amplitude as given by eqs (99), (100) and (104) may penetrate into the slotted cylinder. The results and conclusions we have presented here are in essential agreement with similar theoretical considerations reported on by Oliner and Clarricoats¹⁷ earlier. In their study they considered a slotted circular cylindrical waveguide containing a dielectric rod along its axis. They also chose incidence normal to the cylinder axis, $\theta_{inc} = \pi/2$, and $\phi_{inc} \neq 0$ for a plane incident wave and approximated the actual problem by assuming it to be a quasi-static problem.

17. A. A. Oliner and P. B. Clarricoats, "Transverse Equivalent Networks for Slotted Inhomogeneous Circular Waveguides," Proc. of Inst. Of Electrical Engin. 114, 171 (1967).

The effect of resonance excitation of the slotted cylinder also occurs when $k a \sin \theta_{inc}$ takes on values that are close to the roots of the n -th order Bessel functions $J_n(\)$. This then indicates that the higher order TM modes of the circular waveguide can be excited by incident radiation that has a non-resonant frequency but is incident at an appropriately chosen angle θ_{inc} .

One important point that we have not explicitly developed in detail is the question of the electric field in the aperture itself for $k a \sin \theta_{inc}$ just beyond cutoff of the resonances of the slotted conducting cylinder. Further detailed consideration of the coefficients a_n for $n=0, 1, 2$ as a function of slot angle ϕ_0 and the parameter δ which describes the deviation of $k a \sin \theta_{inc}$ from the actual roots of $J_0(\)$ reveals that the E_z field in the aperture can become appreciable in amplitude. Further it can be shown that as a function of frequency, for example, the amplitude of the z -component of electric field at the center of the aperture reveals a very narrow linewidth centered about some frequency which is quite close to the waveguide resonance for no slot. The maximum amplitude of E_z at the slot center, the linewidth and the central frequency are strongly dependent on the slot angle ϕ_0 .

3. Symmetric, Normal Incidence of E-polarized Radiation.

We have calculated by a high order method of moments approach the tangential electric field amplitude at the center of a $\phi_0=6^\circ$ full length longitudinal slot in a circular cylindrical tube of infinite length. This was done for the direction of incident

radiation corresponding to $\phi_{inc} = \pi$ and $\theta_{inc} = \pi/2$. Thus we are talking about the case of normal symmetric incidence towards the slot. For this situation we have only a z-component of electric field inside and outside of the slotted cylinder and all fields are independent of the z-coordinate.

The results obtained as a function of circumference to wavelength ratio, γ , in the neighborhood of the lowest two modes are shown in figure 2. In the method of moments calculation the conductor was assumed to be approximately described by a roughly equivalent system of $L=200$ conducting strips each carrying its own uniform current. The ratio of each such strip to the half-slot angle it should be noted is

$$\frac{\Delta\phi}{\frac{1}{2}\phi_0} = \frac{(180-3)/100}{3} \approx 0.6$$

which is not a small quantity. On the other hand the ratio of the arclength of each such strip to the wavelength of the incident radiation is

$$\frac{a\Delta\phi}{\lambda} = \frac{2\pi a}{\lambda} \frac{\Delta\phi}{2\pi} = \gamma \frac{\Delta\phi}{2\pi} \approx 0.005\gamma$$

which for the two lowest circular waveguide TM modes is a rather small quantity.

It should be recalled at this point that we have been discussing the ideal situation of an infinitely long, perfectly conducting, infinitesimally thin, slotted circular cylinder. The rather striking

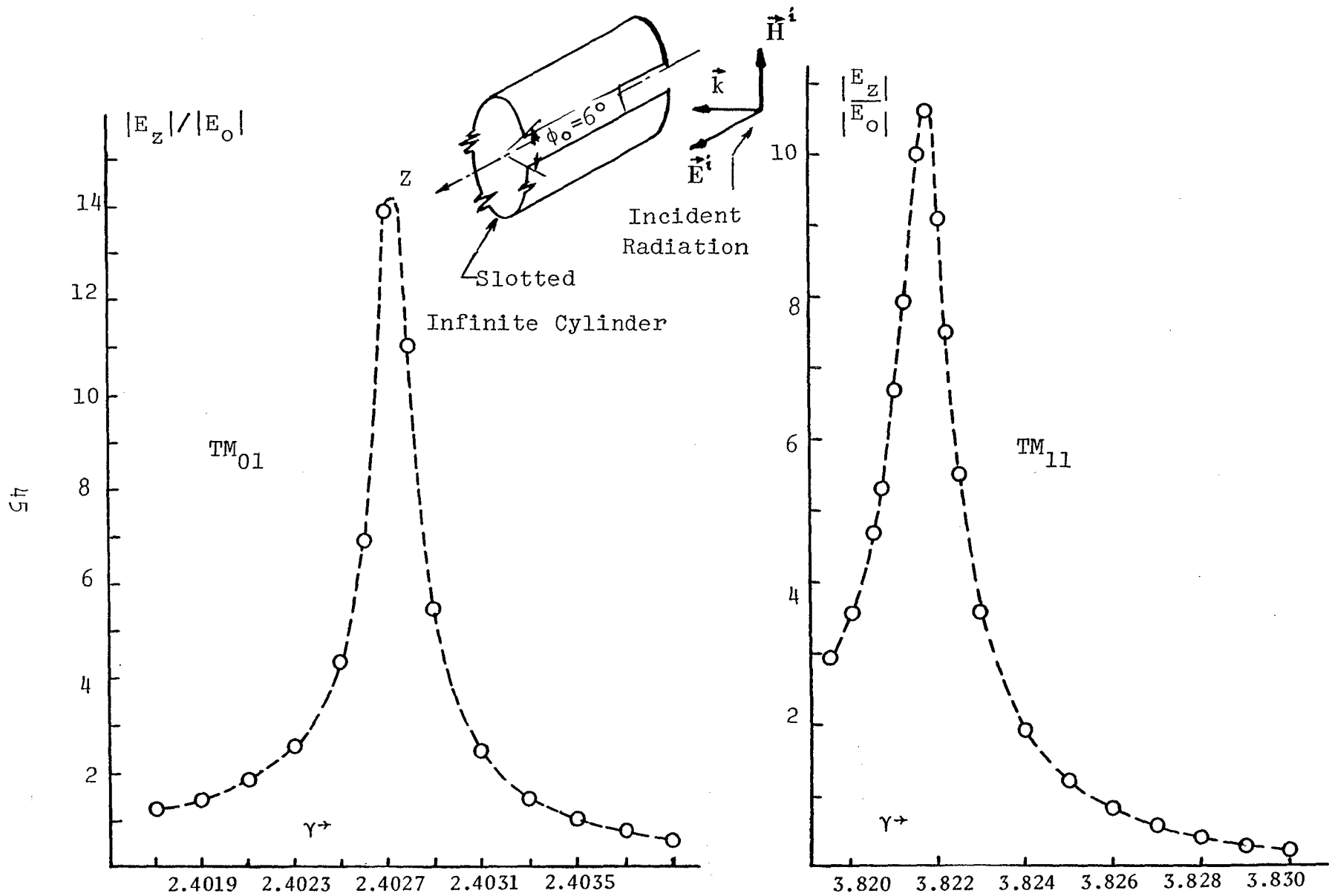


Figure 2. Electric Field Amplitude At Center of Slot In Circular Cylinder For $\phi_0=6^\circ$ Slot and E-polarized Radiation at Normal Symmetric Incidence Near the TM_{01} and TM_{11} Circular Waveguide Modes

aperture fields of figure 2 correspond to that ideal two dimensional diffraction problem. The question very naturally arises as to whether a real three dimensional case of a narrowly slotted thin walled conducting circular cylinder exhibits pretty much the same rather extreme response to similar radiation. To attempt to resolve this question we carried out an experimental program on long, slotted cylinders and investigated the effects of varying the parameters pertinent to the problem. The experimental method will be presented next. After that we shall consider the results obtained in the course of the measurement program.

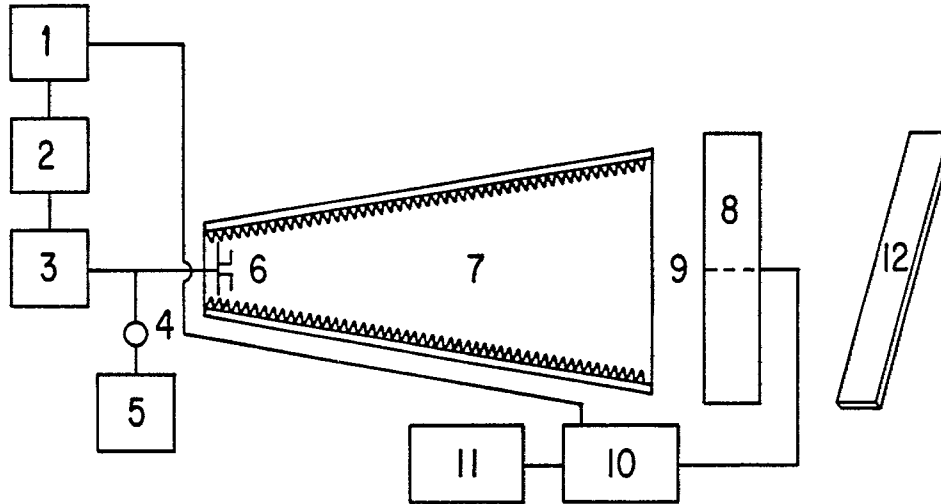
III. THE EXPERIMENTAL METHOD

For the study presented in this report measurements were made with the target cylinder, properly aligned, just outside the large opening of a tapered anechoic chamber. The advantages inherent in using just such a chamber have been adequately described elsewhere¹⁸ and consequently we shall omit the corresponding details from the present discussion. In figure 3 we present a block diagram to illustrate the set-up for the system of measurements. A General Radio Type 1218-B triode oscillator with frequency range from 900 to 2000MHz was utilized as the source of the microwave radiation. From the source the outgoing signal was fed to a dipole antenna which was resonant over the small range of frequency used in this study. This antenna was properly positioned at the small end of the tapered anechoic chamber. In addition to feeding the antenna a small portion of the signal was tapped off to feed a bolometer through a Hewlett-Packard Model 536A frequency meter. By means of this arrangement we were able to obtain measurements of the frequency to five significant figures. Since the resonance peaks involved in the study were generally 1MHz or less in width this degree of resolution for the frequency was required.

The irradiated target cylinders were constructed in a rather convenient and simple manner. A five foot length of Textolite¹⁹

-
18. R. O. Dell, C. R. Carpenter and C. L. Andrews, "Optical Design of Anechoic Chambers," Jour. Opt. Soc. of America, 902, 62 (1972)
 19. Textolite is the trade name of glued fibreboard rolled into cylinders. The cylinders are obtainable from General Electric Co., Schenectady, New York.

BLOCK DIAGRAM OF SYSTEM



- 1 DECADE PREAMPLIFIER
- 2 MODULATOR
- 3 GENERAL RADIO TRIODE OSCILLATOR (.90-2.0 GHz)
- 4 FREQUENCY METER
- 5 POWER METER
- 6 DIPOLE ANTENNA SOURCE
- 7 TAPERED ANECHOIC CHAMBER LINED WITH ABSORBER
- 8 SLOTTED CYLINDER
- 9 SHOTTKY ELECTRIC PROBE
- 10 LOCK-IN AMPLIFIER
11. X-Y RECORDER
- 12 TILTED ABSORBER SCREEN

Figure 3. Principal Components of Measuring System
And Their Interconnections

circular tubing with an outside diameter of 6 1/8 inches (7.779 cm in radius) was used as a form for the metal surface of the required conducting cylinders to be irradiated in the experiment. These cylinder forms are highly transparent to the microwave radiation. Fine lines were inscribed on the Textolite cylinders parallel to one another and to the axis. These lines correspond to various slots which are to be parallel to the axis and subtend slot angles of various sizes from 1° on up. The conducting slotted cylinders were then fabricated by laying down lengthwise strips of aluminum foil scotch tape.²⁰ A small overlap of these strips was allowed. This results in a very thin-walled conducting circular cylinder with, effectively, quite sharp slot edges. These slotted cylinders are of considerable length and should closely approximate in the laboratory the infinitesimally thin, infinitely long, longitudinally slotted conducting cylinder described by theory.

The question of the effects of wall thickness were, in fact, addressed by Koshparenok et. al.¹² They developed a criterion for the wall thickness of the slotted cylinder based on the ratio of the thickness of the wall, Δ , to the width of the slot δ . Their criterion states that the ratio Δ/δ should be less than 0.2 to preserve the stipulation of thin walls given by theory. Now the aluminum foil tape is 0.005 cm in thickness. Then for the smallest slot angle used in the experimental study $\phi_0=1^\circ$ the value of the

20. Aluminum Foil Scotch Tape is a standard commercial product available from 3M Company, St. Paul, Minnesota.

12. V. N. Koshparenok, G. G. Polovnikoff, and V. V. Shestopalov
Ibid.

ratio Δ/δ is 0.018 which quite clearly falls well within the requirements of the thin-wall criterion.

Further comment is in order on the convenience resulting from the use of the foil backed tape. It should be clear that the slot angles, slot lengths and the length of the conducting cylinder itself could be very easily and quite quickly changed as desired merely by adding or removing strips of the metal foil backed tape.

The final part of the experimental set-up to describe is the detector system. An electric field probe consisting of a very small Shottky 5845 diode with copper antenna leads was used to detect the squared amplitude of the electric field component parallel to the detector. The E-field probe is illustrated in figure 4. Extremely high impedance leads from the E-field probe carries the signal to a lock-in amplifier which in turn has output on an X-Y recorder. Because of the small physical size of the electric field probe it has only a minimal perturbing effect on the slot field. An added desirable feature of these probes resides in the important fact that the design is such as to make it possible to manufacture many probes with very nearly identical characteristics. It must also be pointed out that the low internal noise of such an E-field probe makes it an excellent detector for the type of measurement performed in this study. To make a measurement after the desired slotted cylinder is fabricated and carefully aligned with respect to the incident radiation the small electric-field-probe is fixed and aligned at the center of slot in the conducting cylinder and at each frequency $|E_z|^2/|E_0|^2$ is recorded at that position.

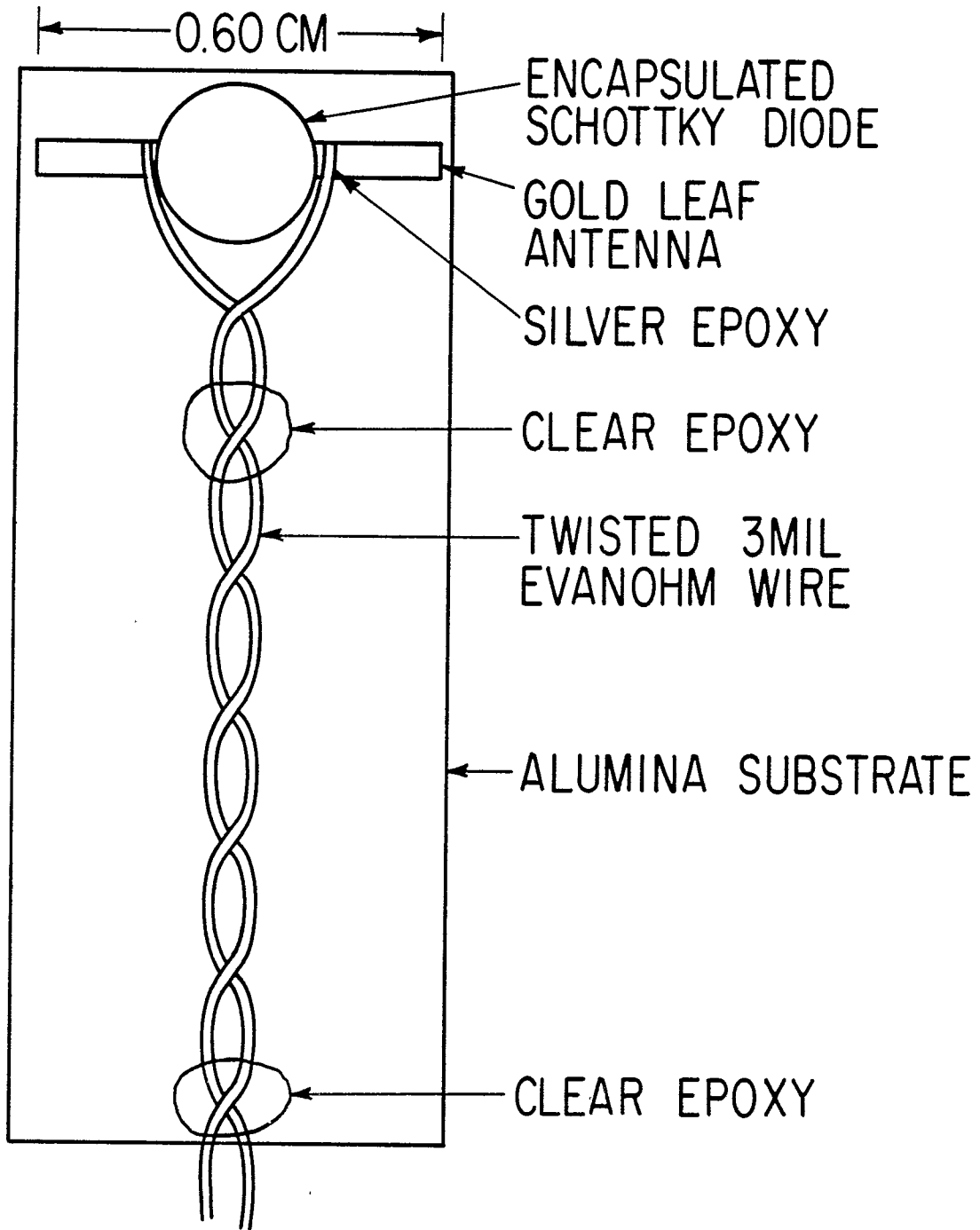


Figure 4. Detailed Illustration of The Electric Field Probe

IV. EXPERIMENTAL RESULTS IN THE TM_{01} REGION

In figure 5 we show the measured amplitude of the longitudinal component of the electric field at the center of a narrow full length slot in a five foot long (152.4cm) thin walled conducting circular cylinder. The incident radiation is polarized with its electric field parallel to the cylinder axis and also to the slot edges. Measured results are shown as a function of circumference to wavelength ratio, γ , or, equivalently, as a function of frequency for several narrow slot angles. The range of frequency represented is a small band in the neighborhood of the TM_{01} mode for the circular cylindrical waveguide in the absence of a slot. This, the lowest mode for the circular cylindrical waveguide, corresponds to the value $\gamma=2.4049$ and coincides with the first root of the zero order ordinary Bessel function of the first kind i.e. $J_0(\gamma_{01})=0$. Also included in figure 5 is the corresponding theoretical frequency dependence calculated for the infinitely long axially slotted circular cylinder for a slot angle $\phi_0=6^\circ$. The theoretical curve is merely that shown earlier in figure 2 and is included in figure 5 to facilitate comparison of the experimental curve for $\phi_0=6^\circ$ with infinite cylinder theory. Let us now examine the data displayed in figure 5. A number of features are quite visible. First we observe that the peak heights increase as the slot angle increases and second the value of γ or frequency decreases simultaneously at the peak value. Further detailed inspection reveals that for all the narrow slots the peak in the electric field at the slot center always occurs

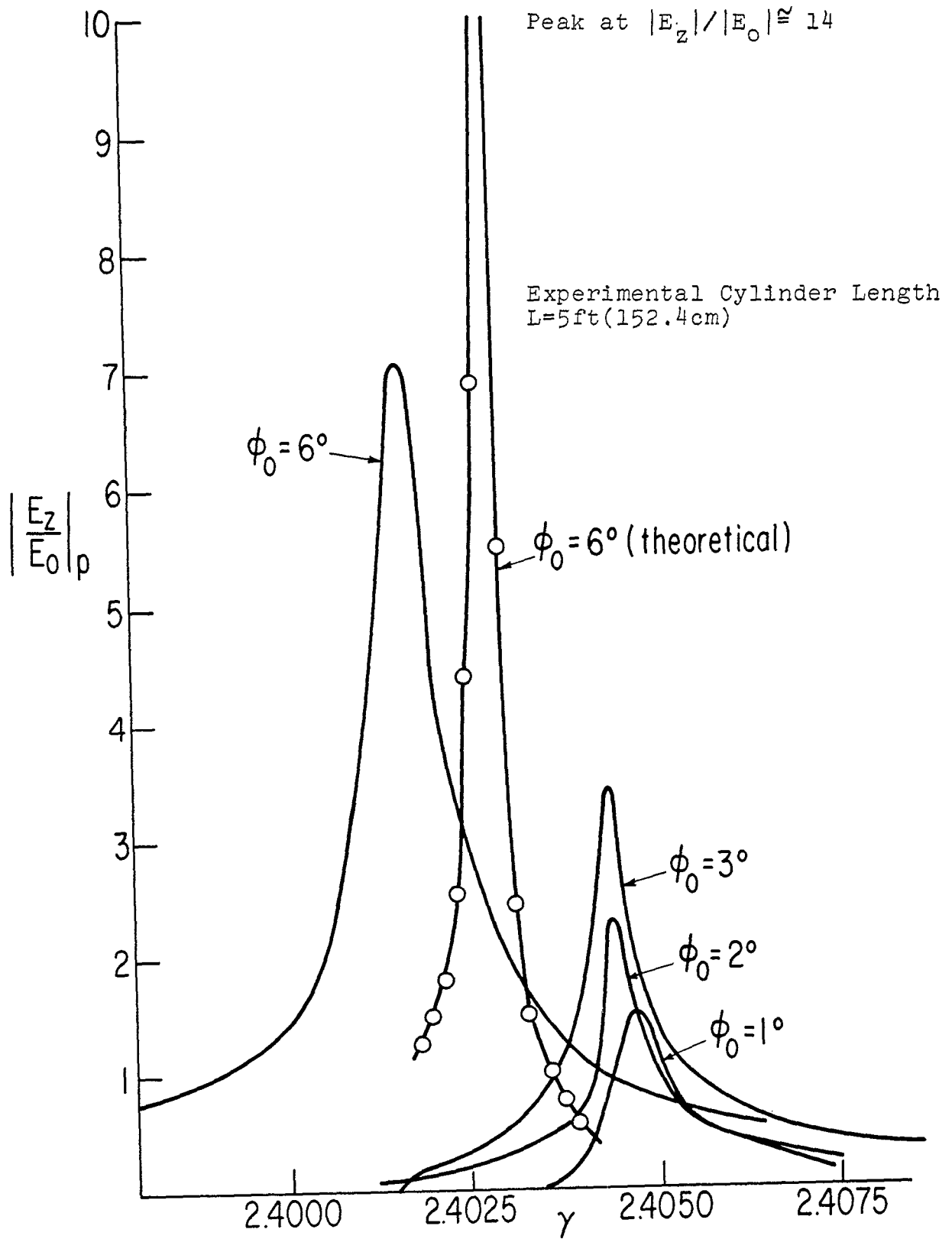


Figure 5. Measured Amplitude of Electric Field at Slot Center Versus γ For Various Slot Angles. The Theoretical Prediction For $\phi_0 = 6^\circ$ Is Shown For Comparison with the Infinite Cylinder

below the natural TM_{01} mode of the unslotted circular cylindrical waveguide. Thus it appears as a result of the experiments that in the presence of a long axial slot in the circular cylinder the lowest natural mode is shifted to lower frequency. Also as the slot is widened this shift downward in frequency is more pronounced. We noted that the theory⁴ earlier predicted such reduction in frequency at all the lower modes for larger slots in the infinite cylinder case. In figures 2 and 5 for narrow slots we observe the theory predicts a down shift for $\phi_0=6^\circ$ consistent with the large slot behaviour for an infinite slotted cylinder. A further characteristic property that appears in figure 5 is the increase in line width around the peak as the narrow slot increases. It thus would appear that we have three primary parameters at hand to describe this resonance effect. These are the γ at the peak height of the line which we shall denote by γ_p , the width of the line centered about the peak which we denote by $\Delta\nu$, and the maximum amplitude or the peak height denoted by $(|E_z|/|E_0|)_p$. Note that the line width is defined as the width in megahertz at 0.707 times the height at maximum amplitude. All the remaining measurements discussed or described below are restricted to only these parameters in order to more compactly and more efficiently obtain the relevant characteristics associated with the experimentally observed resonance lines. After the detection of such a line by sweeping over the frequencies the central frequency and its corresponding amplitude could be measured simultaneously.

4. L. F. Libelo, A. G. Henney, J. N. Bombardt and F. S. Libelo.
S.E.R.A. X op.cit.

Then, since the recorder indicated the measured intensity for the field, the frequency could be adjusted until the recorder read half of the intensity at maximum. The corresponding frequencies could then be recorded for such points on either side of the peak or central frequency. The difference between these two frequencies gives the peak width $\Delta\nu$ we have just defined. Results obtained from measurements taken at the maximum amplitude for additional values of slot angle in the full length slotted 5 ft (152.4cm) cylinder are shown in figure 6. In this figure we can quite clearly discern a well behaved monotonic decrease in γ_p or central frequency as the slot angle is allowed to widen out. This characteristic behaviour persists up until the slot angle becomes about equal to $\phi_0 \approx 20^\circ$. Further increase in ϕ_0 results in considerable difficulty in clearly establishing the location of the peak amplitude. It would appear that at this point we have experienced a transition of sorts from narrow slots to intermediate slot angles. This is consistent with our earlier experience with the theory for the infinite axially slotted cylinder⁴ and with measurements obtained on finite axially slotted cylinders.^{21,22} Evidently the line for TM_{01} has broadened sufficiently and dropped substantially in amplitude to become rather poorly defined for our finite system. Figure 7 gives the experimentally obtained behaviour of the linewidth for TM_{01} as a function

-
4. L. F. Libelo, A. G. Henney, J. N. Bombardt. S.E.R.A. X. op. cit.
 21. L. F. Libelo, J. P. Heckl, C. L. Andrews, D. P. Margolis. 1975 IEEE International EMC Symposium Record, Oct 1975, San Antonio, Tx.
 22. D. P. Margolis. Ph.D. Dissertation Department of Physics, State University of New York at Albany, N. Y. 1976.

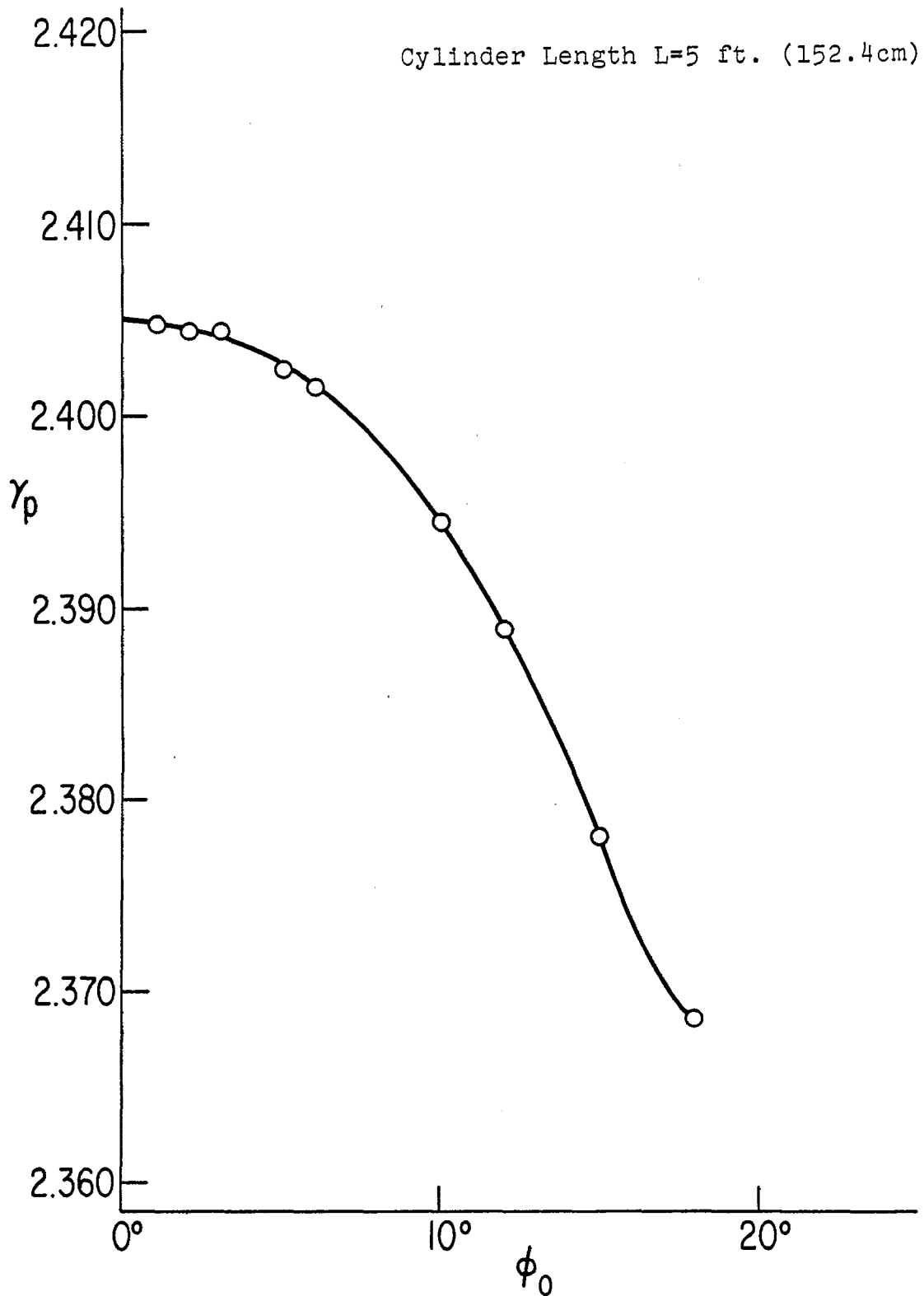


Figure 6. The Measured Value of γ At Peak Maximum versus Slot Angle Using the Five-Foot (152.4cm) Long Slotted Cylinder

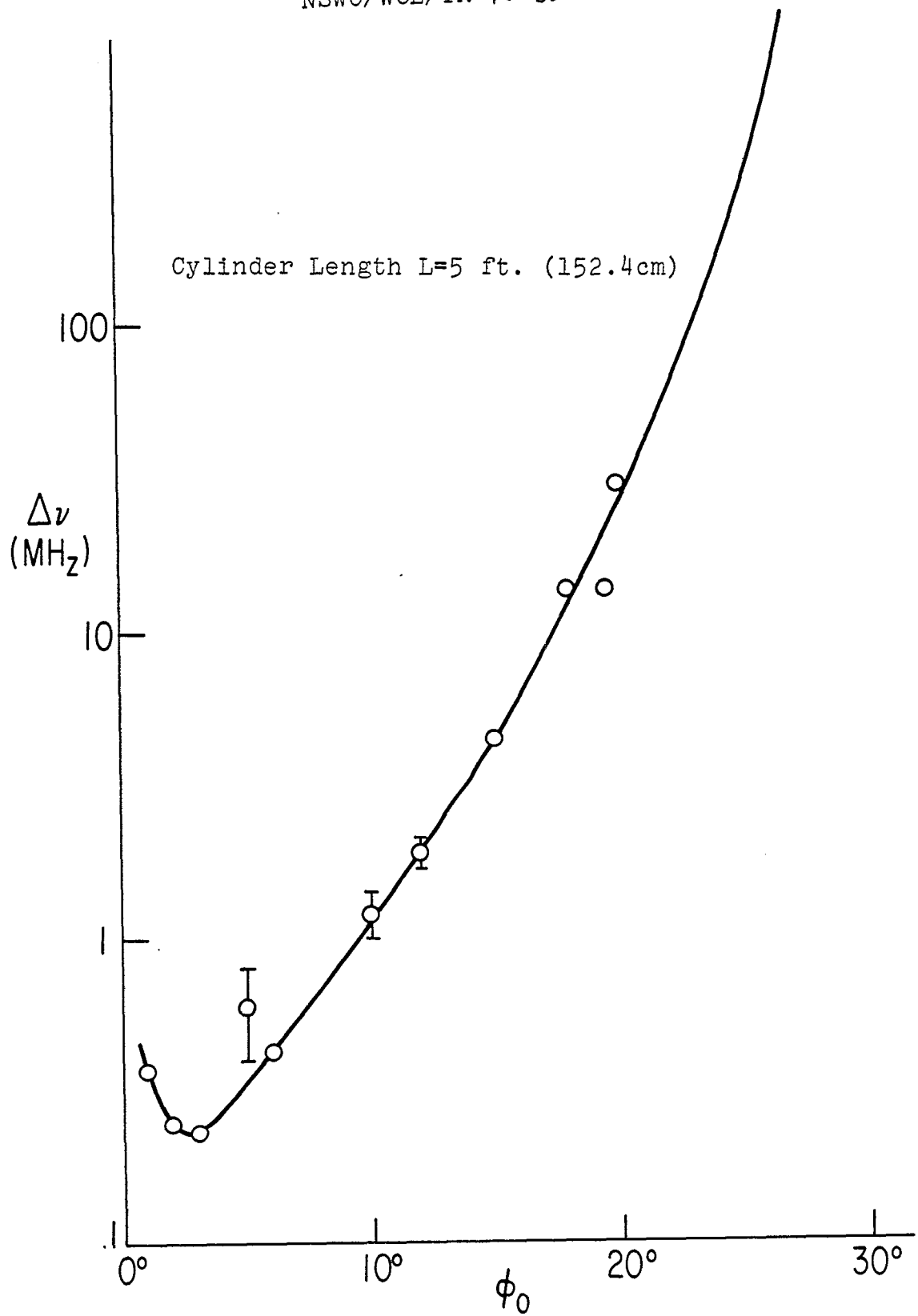


Figure 7. Measured Linewidth of the Amplitude of the Longitudinal Electric Field at the Center of the Slot as a Function of Slot Angle

of slot angle. We see quite plainly that from about $\phi_0 \approx 3^\circ$ a smooth but rapid increase in Δv occurs as ϕ_0 increases to about 20° . We have merely extrapolated the empirical curve beyond $\phi_0 \approx 20^\circ$. The apparent minimum at $\phi_0 \approx 3^\circ$ is basically the result of experimental uncertainty at the very small slot angles. Consistent with what we have just seen displayed as the behaviour of γ_p and Δv we find in figure 8 that the measured maximum amplitude $(|E_z|/|E_0|)_p$ near TM_{01} increases with increasing slot angle to a substantial maximum at about $\phi_0 \approx 10^\circ$. Further increasing the slot angle results in a decrease in peak height at the slot center. This behaviour continues until a slot angle size of about 20° is attained. Collectively figures 6, 7 and 8 strongly suggest, on empirical grounds, the occurrence of a more or less well defined bound on what size slot can be safely considered as a narrow slot. For TM_{01} at least this is established. Since the difference between small and large depends upon the wavelength this transition property still remains to be investigated in appropriate detail for the higher order modes.

Before proceeding with the discussion we pause temporarily to point out the degree of complexity of the problem at hand. We have in the laboratory the following situation to investigate; namely, a system characterized by, $2\pi a/\lambda$, a parameter giving the circumference to incident wavelength ratio, L_0/λ , a parameter fixing the cylinder length to wavelength ratio, $a\phi_0/\lambda$, a parameter giving us the slot arc length to wavelength ratio-which we are constraining to be small-and what would seem to be the last parameter L_s/λ

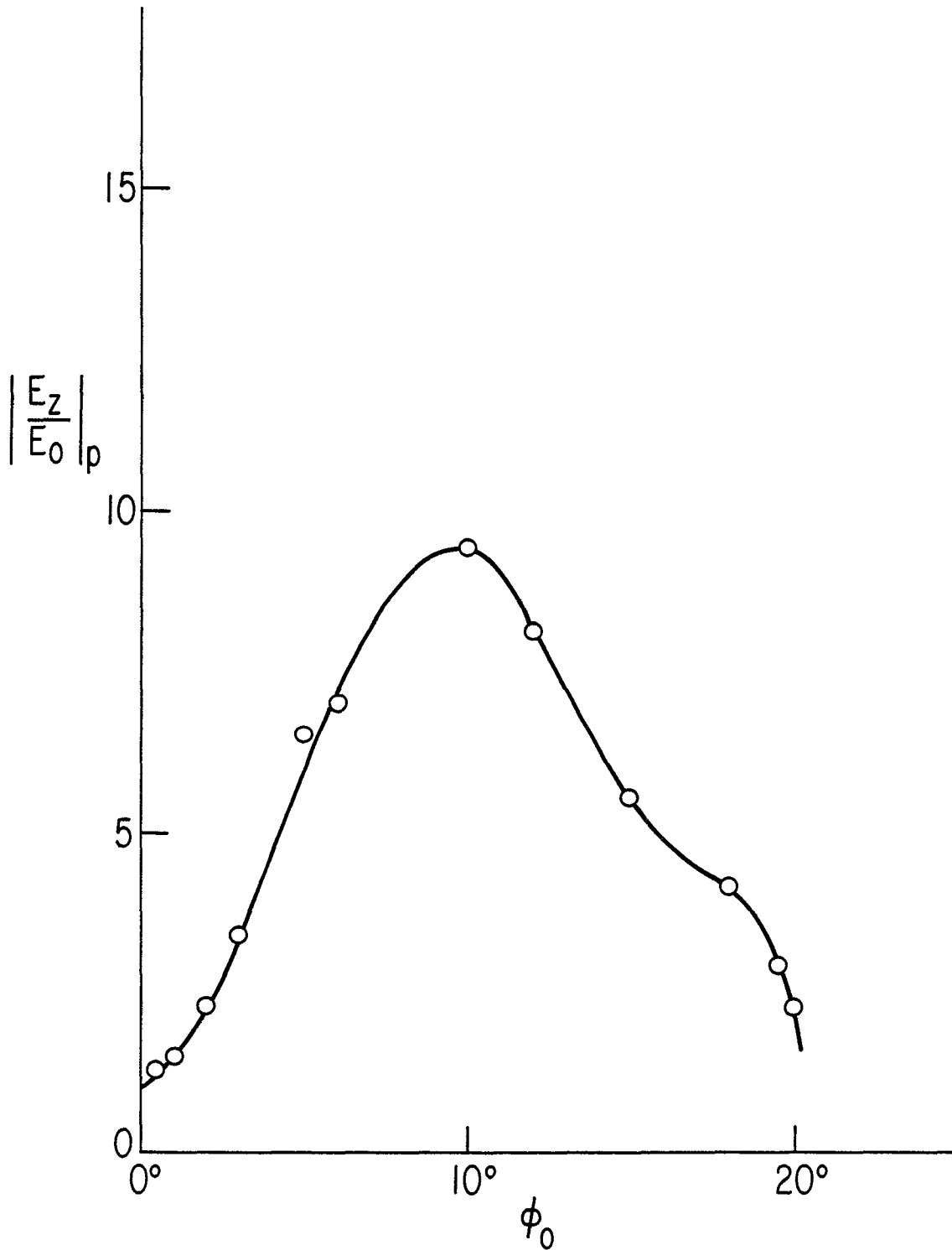


Figure 8. Measured Peak Amplitude of Electric Field at the Slot Center As a function of Slot Angle For 5ft(152.4cm) Long Cylinder With Full Length Axial Slot.

which gives the slot length to wavelength ratio. Of course thus far we have only seen empirical results for $L_s/\lambda=L_o/\lambda$. It should be kept in mind that for normal symmetric incidence on the slot of E-polarization there are at least three possible cases to consider; namely, the slotted finite cylinder is fully open at both ends, fully open at only one end, or fully closed at both ends. We are, of course, considering here only the situation for both ends fully open. Of the vast number of possibilities we are severely restricting our specific study to encompass a highly selective combination of the parameter ranges. The measurements obtained and presented in this report are the first such empirical data. Consequently, we shall discover, not surprisingly, some new and quite interesting properties and many familiar characteristics revealed by the experimental investigation. With these comments in mind let us again return to the presentation of the results of the measurements.

Before we comment on comparison of the theoretical prediction of the infinite axially slotted cylinder characteristics to those measured for the finite but fully slotted cylinder for the same slot angle we first present results obtained experimentally as a function of slot length. In figure 9 we present the measured results for the peak value of γ as a function of the length L_s of the finite axial rectangular slot scaled in units of the wavelength at maximum amplitude λ_p . Results are displayed for three slot angles $\phi_o=6^\circ$, 10° and 15° . We find, not unexpectedly, that as the scaled slot length decreases all three curves for γ_p approach the consistent

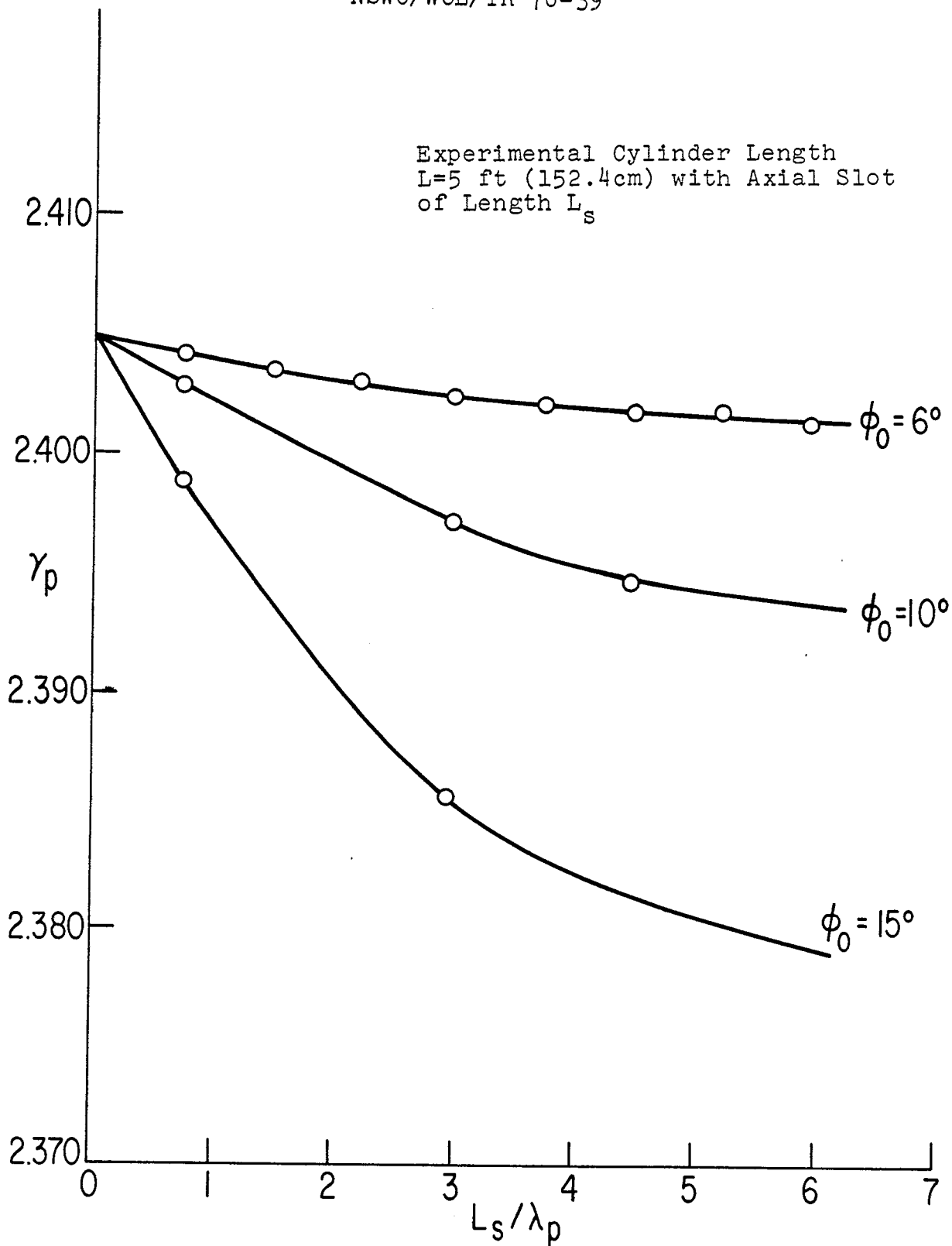


Figure 9. Measured Value of γ At Peak Versus Slot Length In Units of Wavelength At Peak For Various Slot Angles

common value γ_{01} for the lowest mode of the infinite circular wave guide without a slot. Also as we should expect for larger slot lengths the larger the slot angle the lower the measured line peak occurs. It should be noted that λ_p varies in figure 9 by only about 1 to 2% as can be seen from figure 6. Proceeding in the other direction we should expect that as the slot length increases γ_p should asymptotically approach the corresponding infinite slotted cylinder value. This is certainly the case for $\phi_0=6^\circ$. Although the theoretical results are not explicitly shown for $\phi_0=10^\circ$ for the infinite cylinder this also happens to be the case. For $\phi_0=15^\circ$ we can only speculate that this again holds true in the asymptotic limit. It should be kept in mind that even though the slot length L_s is being varied in figure 9 the actual cylinder length is being maintained at $L_0 = 5 \text{ ft}(152.4\text{cm})$. For this reason we cannot realistically continue to increase L_s to obtain a clearer picture of the asymptotic behaviour of γ_p versus L_s for the larger slot angles. At $\phi_0=15^\circ$ this is already evident in figure 9. Figure 10 shows the line width as a function of slot length, scaled in units of wavelength at peak, as measured for the slots with $\phi_0=6^\circ, 10^\circ$ and 15° . Note that the vertical scale is logarithmic. For the larger slot angles we have a nearly linear behaviour for the line width as a function of L_s/λ_p with a decrease in Δv showing up as L_s decreases. The larger slot angle at fixed L_s/λ_p has as expected the larger line width. Also the larger slot angle gives rise to the larger slope for Δv versus L_s/λ_p . Although the behaviour for the smallest

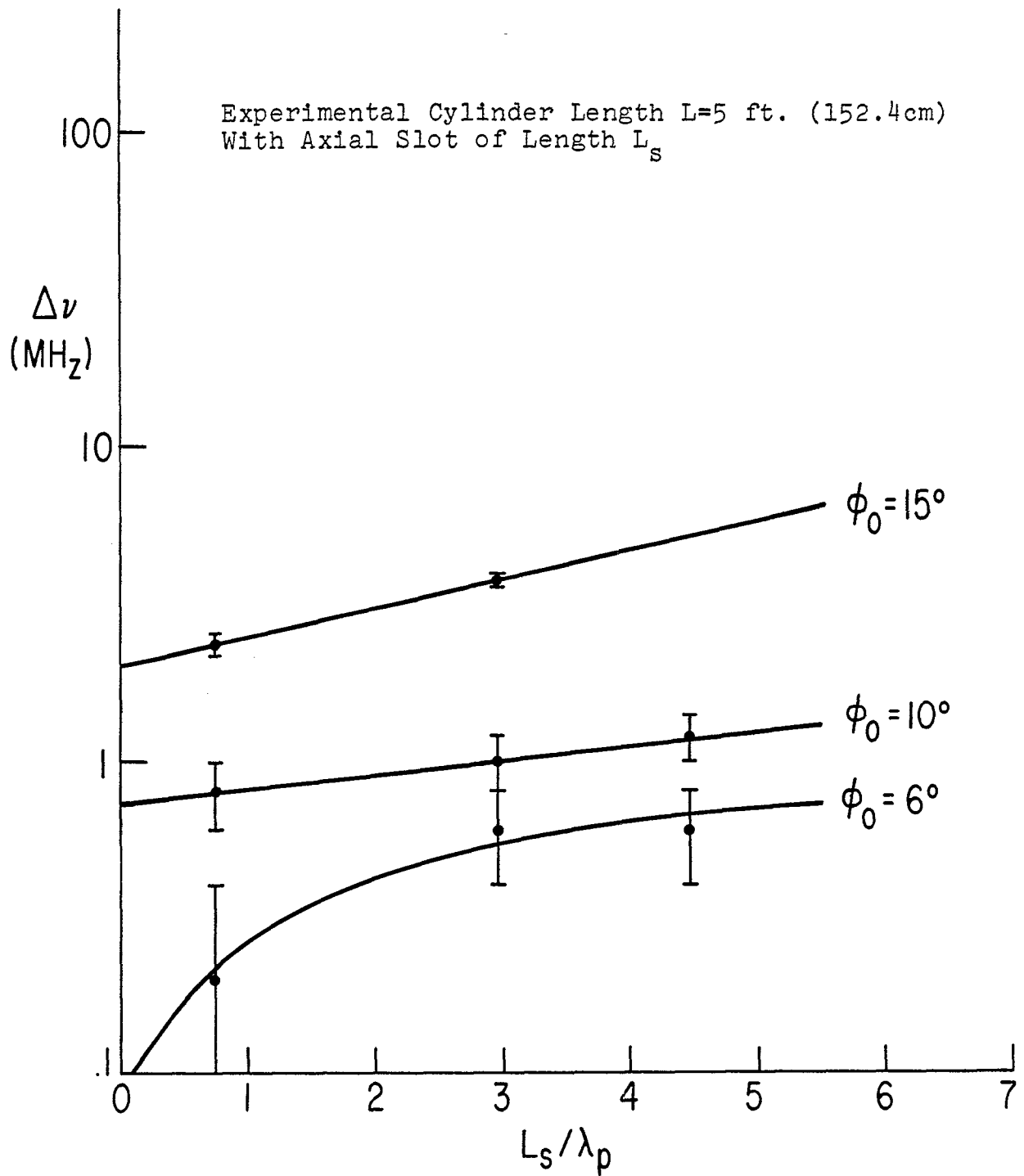


Figure 10. Measured Linewidth Versus Slot Length In Units of Wavelength at the Peak Value of Slot Field For Various Slot Angles.

slot angle $\phi_0=6^\circ$ is consistent with the larger ϕ_0 cases we unfortunately have too large an experimental uncertainty to clearly see the behaviour of very small slot lengths in the cylinder of fixed length L_0 . Except for very short rectangular slots of very small slot angle we have a straightforward technique of determining the line width. We are now considerably improving the instrumentation to rectify this limiting characteristic. The variation of the peak height $(|E_z|/|E_0|)_p$ as a function of axial slot length in units of wavelength at peak amplitude is shown in figure 11 for slot angles $\phi_0=6^\circ$, 10° and 15° . Within the limits inherent in the fixed length of the slotted cylinder we observe that for the longer axial slots the peak height is larger for the narrower slots. As the scaled slot length decreases the measured peak height decreases for all three slot angles. An interesting feature is evident in figure 11. We observe that as L_s decreases the peak height for $\phi_0=6^\circ$ decreases most rapidly and eventually lies below that for 10° and 15° . Further decrease in slot length then indicates that the peak height for $\phi_0=10^\circ$ rapidly attenuates and eventually lies below that for $\phi_0=15^\circ$. Thus for small slot lengths we appear to have an inversion. Whereas for long slots the narrower slot angle leads to a higher peak in the slot field at slot center, we observe that at very short slot lengths the peak height is lower for the larger slot angle. Note that the general peak height is lower at short slot lengths than for the longer slots. The long slot behaviour observed is consistent with that for the infinite slotted cylinder with full length slot as

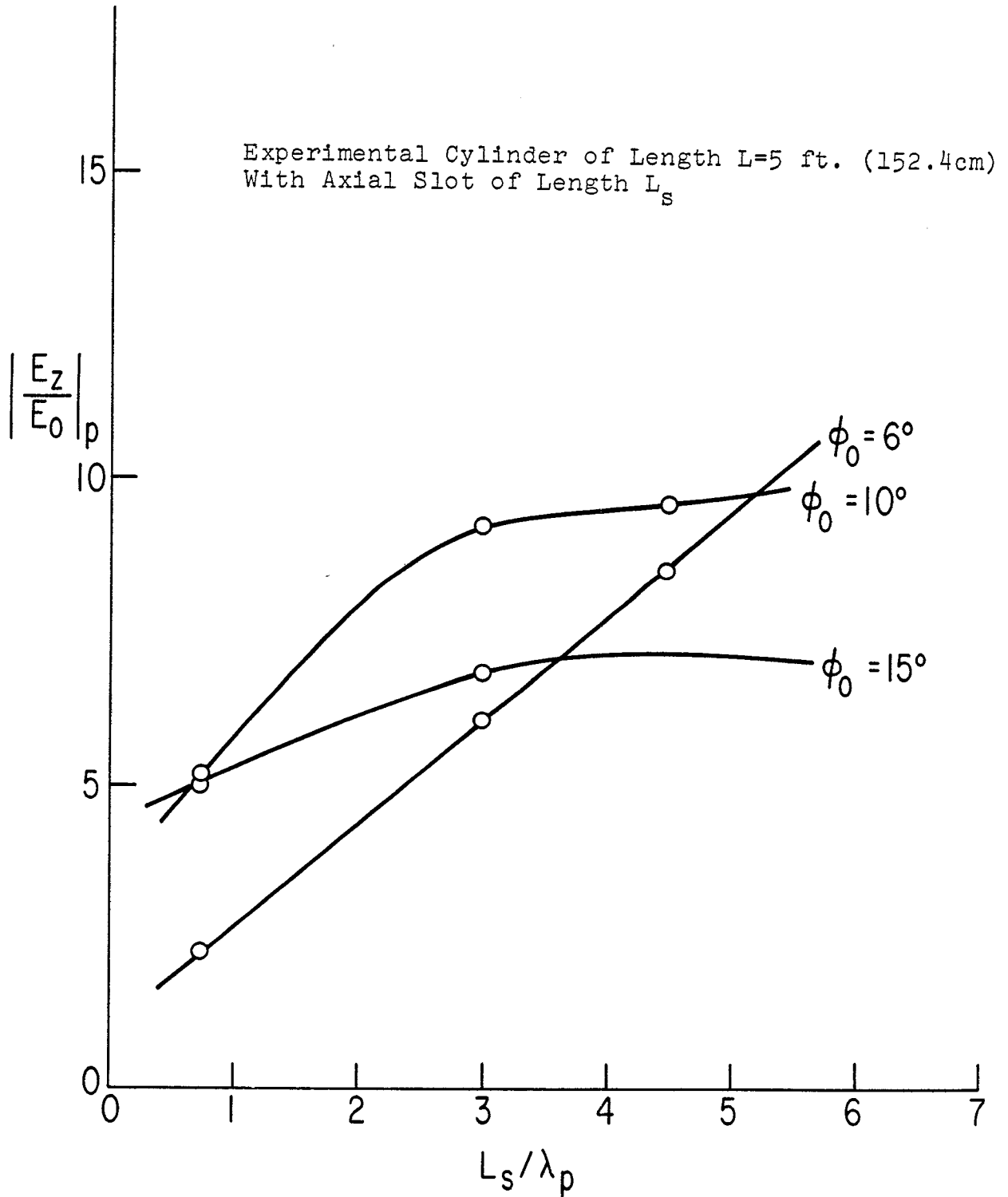


Figure 11. Measured Peak Amplitude of Electric Field at Slot Center Versus Slot Length In Units of Peak Wavelength For Various Slot Angles

predicted by the theory. This is an essential point to note. From examination of figure 11 it can be seen that the measured peak height for $\phi_0=6^\circ$ is still increasing at a substantial rate at the larger slot lengths. Very likely increasing the basic length of the cylinder i.e. L_0 and then L_s in turn will eventually cause the peak height to turn and level off and come into better agreement with the ideal theoretical prediction.

The effect of cylinder lengths, L_c , shorter than the reference length, $L_0 = 5 \text{ ft}(152.4 \text{ cm})$, as determined by measurement is next considered. Figure 12 shows the measured value of γ at peak height as a function of cylinder length L_c in units of the reference length L_0 for several slot angles. The slot length is now $L_s=L_c$ again. We immediately observe upon inspection that for a given slot angle ϕ_0 decreasing the length of the fully slotted cylinder very plainly shifts the γ at peak height or, equivalently, the central frequency of the resonance line to higher values. This increase is more rapid the shorter the slotted cylinder. We further observe that γ_p for a fixed length is larger the smaller the slot angle ϕ_0 . Then as far as establishing the central frequency of the resonance line is concerned we note that we can either keep the length fixed and decrease the slot angle or alternatively keep the slot angle fixed and decrease the length and produce the same γ_p . For the range of L_c/L_0 and ϕ_0 in figure 12 these variations are essentially equivalent means of tuning to a given γ_p . We also note in figure 12 that, for all the narrow slot angles considered, increasing the cylinder length

beyond L_0 , the reference length, will eventually cause the rate of change of γ_p to slow down and γ_p will then asymptotically approach some definite fixed value a different one for each slot angle ϕ_0 . It should be clear that as we decrease the cylinder length L_c we should not expect the exact infinite cylinder resonances to remain as characteristic of the finite cylinder modes. This is reflected in the rapid change in γ_p as L_c decreases significantly. Ramo, Whinnery and Van Duzer,²³ for example, point out that as far as the distribution of the internal fields and internal side wall surface currents are concerned the infinitely long circular cylindrical ideal waveguide at TM_{01} is identical with the circular cylindrical ideal cavity, of length L_c , resonating in the TM_{011} mode. This is true providing the radii are equal. They further give the expression for cavity resonance wavelength i.e. for γ_p in terms of the cavity height and the wavelength at cutoff, λ_c , for the mode. This relation is precisely

$$105) \quad \lambda_p = \frac{L_c}{\sqrt{0.25 + (L_c/\lambda_c)^2}}$$

where $\lambda_c = 2\pi a/2.4049$. The corresponding value of γ_p for eq (105) has been calculated as a function of cavity height and the results are shown in figure 12 and labeled the "Theoretical Curve" corresponding to the slot angle $\phi_0=0^\circ$. Because of the very close

23. S. Ramo, J. R. Whinnery and T. VanDuzer, "Fields and Waves In Communication Electronics," Section 10.08, J. Wiley & Sons, Inc., New York, 1965.

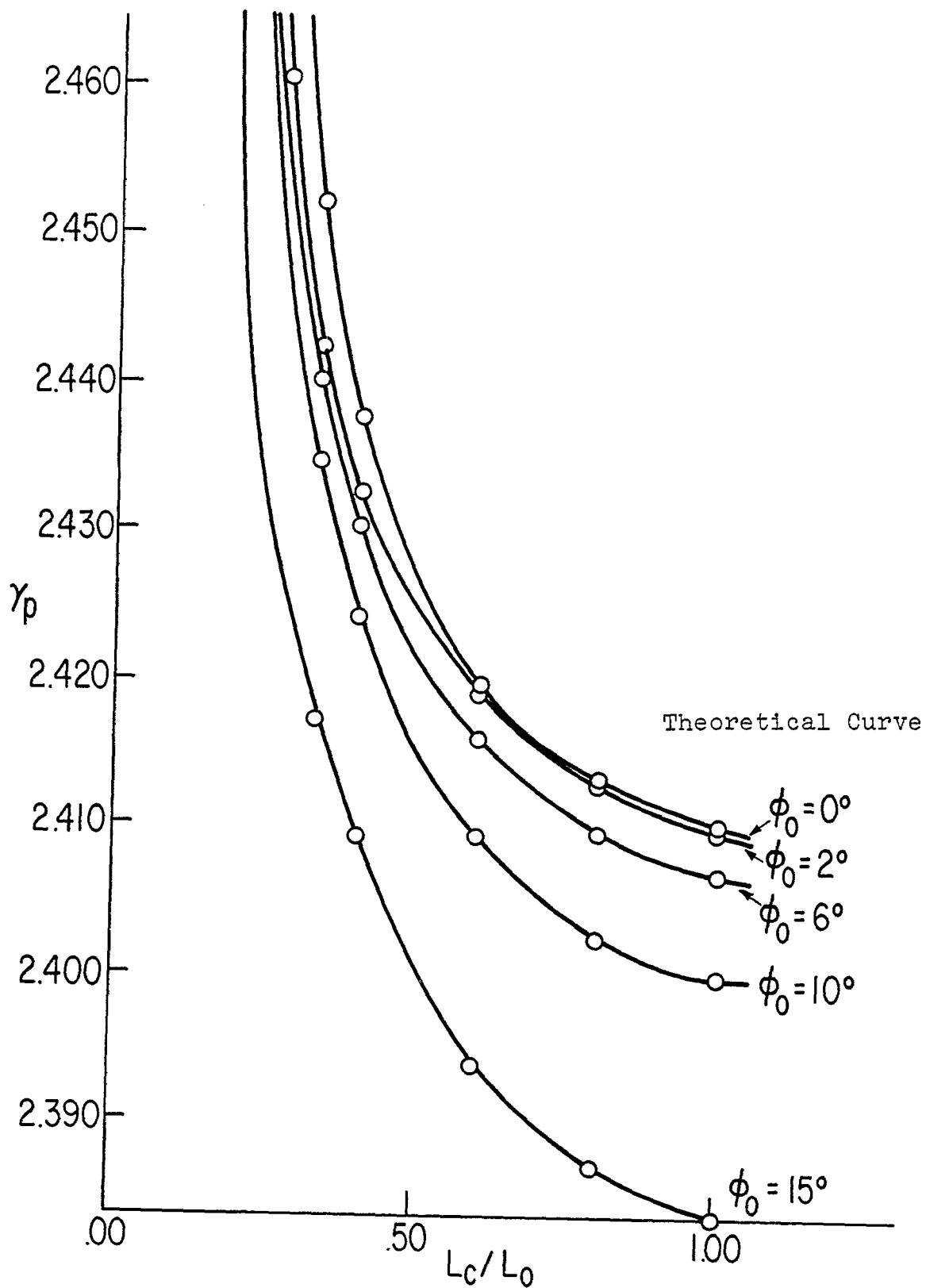


Figure 12. Measured Values of γ At Peak Versus Cylinder Length In Units of Reference Cylinder Length $L_0=5\text{ft.}(152.4\text{cm})$ For Various Slot Angles

resemblance the internal fields to be expected in the very narrow slotted cylinder, far from the ends, bear to the corresponding internal fields in the closed cavity the analytic relation in eq (105) provides a convenient bound on the experimental curves of the type displayed in figure 12. In figure 13 we present the results obtained for the line widths as a function of cylinder length (in units of the reference length L_0) for several full length slots of small angle. Although the behaviour exhibited is somewhat complicated we nevertheless can discern some systematic characteristics. We observe for example that except for the very short fully slotted cylinders the larger the slot angle the broader the line is for fixed cylinder length. Also we see that as the cylinder length, L_c , decreases the line width increases. This is not surprising since the resonance lines become considerably less distinct as the cylinder itself becomes less infinite-like. The peak amplitude of the electric field at the center of the slot is shown in figure 14 as a function of the length of the cylinder (normalized to the reference length L_0). Results obtained for several slot angles are shown. The behaviour of the curves is much more complex than anything we have found thus far. What we observe for all slot angles studied is an increase in peak height at slot center as the cylinder length decreases. Continued shortening of the slotted cylinder then results, at about the same value of L_c , in a sharp decline in the peak field at the center of the slot. At about $L_c/L_0 \approx .03$ the peaks become increasingly difficult to resolve. We can make one

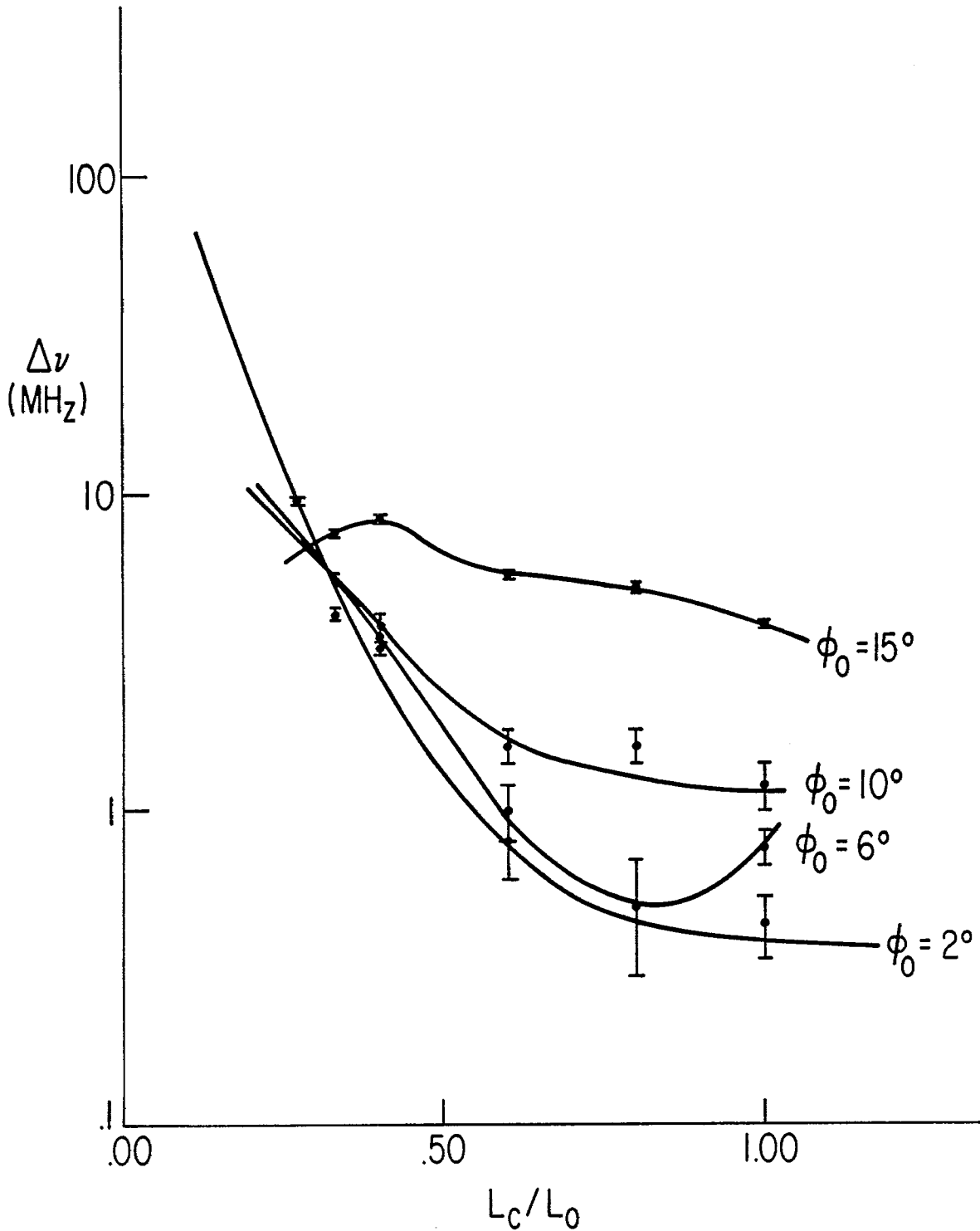


Figure 13. Measured Linewidth As a Function of Cylinder Length L_c
 In Units of the Reference Cylinder Length $L_0=5$ ft(152.4cm)
 For Various Slot Angles

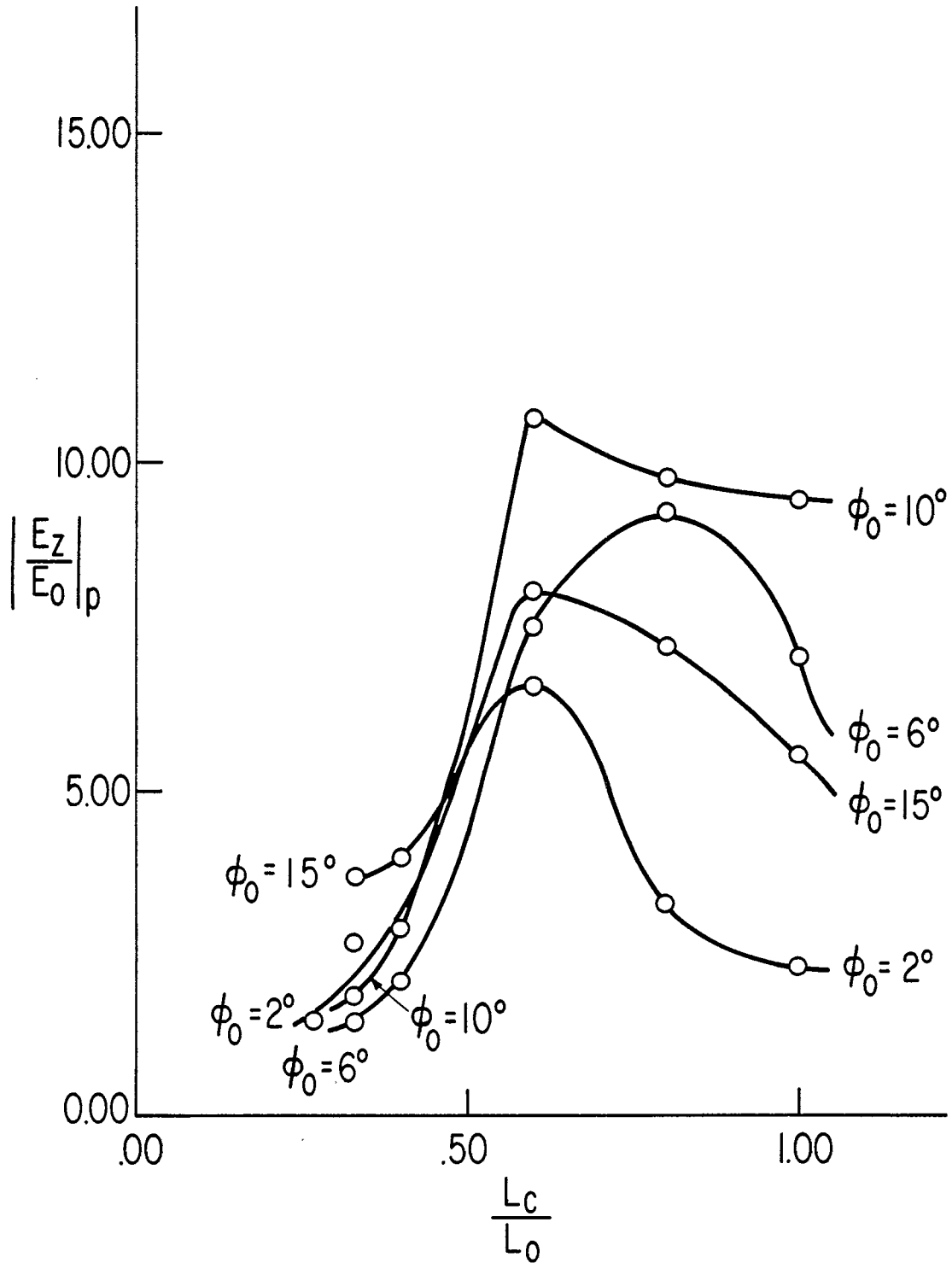


Figure 14. Peak Amplitude of Electric Field At Slot Center Versus Cylinder Length L_c In Units of Reference Cylinder Length $L_0 = 5$ ft (152.4cm) For Various Slot Angles

important point concerning the question as to how well the field at the slot center can be represented by the infinite cylinder field there. The reference length chosen in the experimental study L_0 is about 75 wavelengths long compared to the $\gamma_{01} = 2.4049$ wavelength. Then to achieve agreement to five significant figures with the infinite cylinder theoretical predictions at the slot center we must have a finite cylinder of length L_0 at least 100 wavelengths long and the slot must be just as long.

Figure 15 gives us another view of the central frequency or γ at peak amplitude as a function of slot angle ϕ_0 . The measured results are shown for several slot lengths (in units of the reference cylinder length L_0) in the reference cylinder. Here we see quite clearly that for a given slot angle the central frequency of the resonance line shifts down in frequency more for a longer slot. In all three cases of slot length we find that as the slot angle decreases the central frequency approaches the same limiting value. We again note that somewhere in the neighborhood of the value $\phi_0 \approx 20^\circ$ we find characteristics of a transition between small and intermediate slot angles. For such values of ϕ_0 and larger the curves in figure 15 will flatten out with increasing slot angle ϕ_0 . Where this turning point occurs depends on the slot length L_s .

In figure 16 we have displayed the actual measured values of γ at the central frequency of the resonance line as a function of the slot angle ϕ_0 . The data is shown for several values of slotted cylinder length L_c (in units of L_0). In each case the experimental

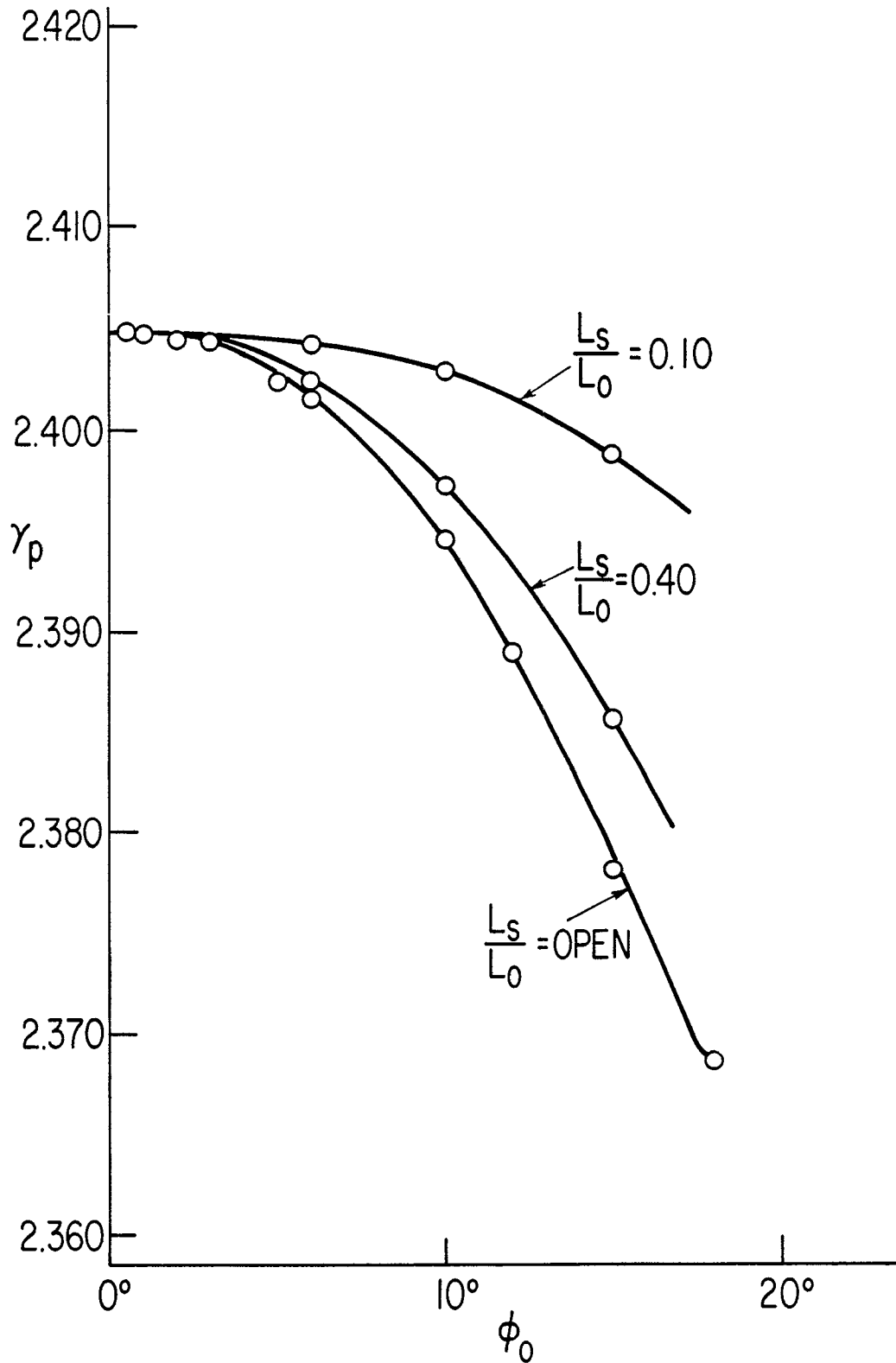


Figure 15. Measured Values of γ At Peak Aperture Field Versus Slot Angle For Various Slot Lengths L_s in Units of Reference Length $L_0 = 5$ ft (152.4 cm)

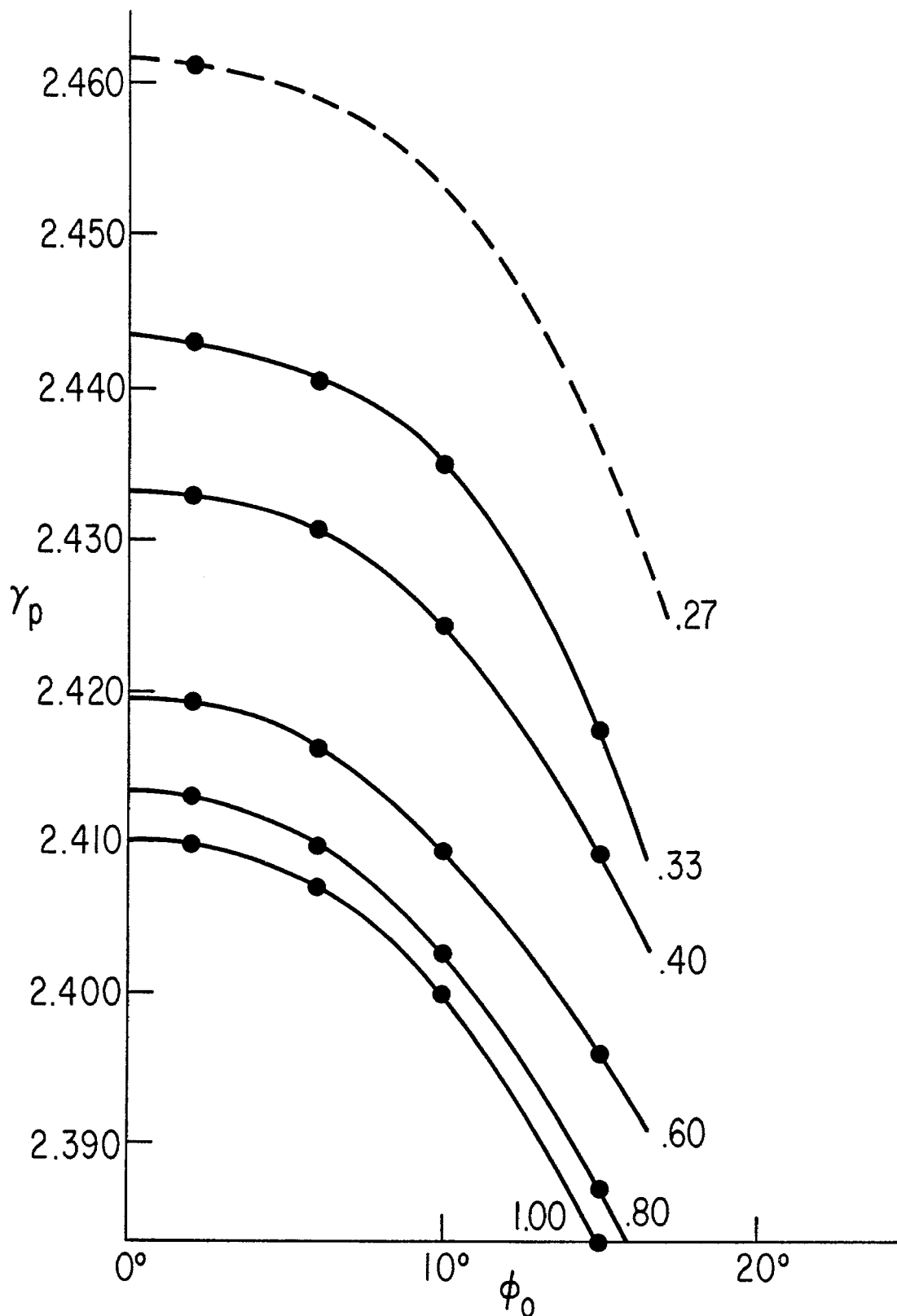


Figure 16. Measured Values of γ At Peak Slot Field Versus Slot Angle For Various Cylinder Lengths L_c in Units of Reference Cylinder Length $L_0 = 5\text{ft}(152.4\text{cm})$

curve was extrapolated to the $\phi_0=0^\circ$ limit. If however we use eq (105) to calculate a γ_p for each L_c and assume it corresponds to the case $\phi_0=0^\circ$ we find the measured data extrapolated to $\phi_0=0^\circ$ do not coincide with the corresponding value calculated via eq (105). These discrepancies were found to be rectified by correcting for a slight variation in the angle of incidence in the experiment. The ratio of the extrapolated data at $\phi_0=0^\circ$ for the cylinder lengths L_c to the calculated values using eq (105) gave a resulting factor $\sin\theta_{inc}$ such that $\theta_{inc}=82.664^\circ$ to within a tenth of a percent. When this error is corrected for we find that the infinite length γ agrees with $\gamma_{01}=2.4049$ to five significant figures. After this was first taken into account the previous experimental curves of figures 5 through 15 were plotted. Also it should be noted that the dashed line in figure 16 for $L_c/L_0=0.27$ is the estimation for the corresponding curve for a relatively short cylinder and has been drawn through one experimental point taken for $\phi_0=2^\circ$.

One further point must be emphasized here. This is the question of the effect that the physical size, although it is quite small, of the electric field probe sitting in the center of the slot has on the reading of the amplitude of the field at the slot center. Because of its size it is reading an average of the field over a small but finite area of the slot which of course does include the slot center. This tends to reduce the amplitude measured there. For narrow slots this effect may not be negligible. It could account for an appreciable amount of the difference seen in figure 5 between what we

have called the measured line at the slot center and the theoretical line we calculate at the center of an infinite system. Measurements are being planned to investigate this experimental limitation by reducing the sensor in size and also by changing its position to see the effect it has on the actual field at the center of the slot in a finite length cylinder. Furthermore we are planning to consider longer finite cylinders to assure convergence toward the infinite system limit.

V. SUMMARY

We have analytically investigated the case for a narrow angle, full length, axial slot in an infinite, circular, thin walled, ideally conducting cylinder. For E-polarized radiation and incidence at arbitrary angle θ_{inc} relative to the cylinder axis of symmetry we have shown that a potentially hazardous energy density can build up in the central region of the narrow slot for effective frequencies in the incident radiation that correspond to natural waveguide modes for the slot-less circular cylindrical waveguide. Since a buildup of this type can be readily dumped into the interior of the slotted cylinder it implies the likelihood of the coupling to enclosed components, in the broad sense, of an undesirably large amount of energy. The concomitant consequences of coupling large quantities of radiant energy at long wavelength through a narrow opening in what should have been a good shield at such wavelengths are manifold. Clearly these consequences are predominantly unpleasant and indeed this problem is somewhat a surprising one. It should be emphasized that a sudden perturbation of the situation at high energy buildup in the narrow slot can serve as the mechanism for dumping the energy into the interior where it can interact with whatever is available for it to couple with. We have in fact experienced in the laboratory, for finite length cylinders of course, just such perturbations which do indeed result in a sudden penetration of the electromagnetic energy into the cylinder through the narrow aperture. It should be recalled that the theoretical development above has also revealed that even for incident radiation at frequencies not coincident with the

natural modes of the circular waveguide it is possible to excite those modes. This we saw can be achieved by arranging for the direction of incidence to assume the appropriate value for θ_{inc} . As a result of this property we find again a somewhat unexpected situation in which a possible hazardous situation can result in a narrow slotted cylindrical shield. The amplitude of the electric field at the center of the narrow slot for $\phi_0=6^\circ$ was explicitly calculated for normal symmetric incidence on the slot so as to obtain the frequency, or γ , dependence in the neighborhood of the lowest two circular waveguide modes, TM_{01} and TM_{11} under the best symmetry conditions. These results were obtained utilizing the STEPS program, described in S.E.R.A. V³, in a high order mode of the Method-of-Moments calculation. The large field at the central frequencies and the narrow line widths that were obtained make manifest the analytic predictions for the field buildup at the slot center.

To establish the extent to which the large field or high energy density buildup in a narrow angle rectangular axial slot occurs in the three dimensional problem of a finite but long cylinder we have pursued an experimental program to investigate the situation. Although the measurements were restricted to the case of E-polarization of normal symmetric incidence on the slot the effects of varying the slot angle ϕ_0 , the slot length L_s and the cylinder length L_c on the linewidth, peak height and central frequency (or γ_p) were obtained

3. J. N. Bombardt, L. F. Libelo, S.E.R.A. V. op. cit.

but only near the TM_{01} mode for the circular waveguide.

The sum total of the experimental results seems to support the anxiety raised by the theoretical predictions for narrow slots in infinite cylinders. Although we find upon inspection of figure 5 that the measured peak field seems to be about half that of the predicted field in the ideal case it must be kept in mind that the probe used in the measurement is probably masking the true amplitude and indeed the real field in the real system may be quite large and quite close in distribution to the ideal case.

In closing we point out that we have presented the first extensive set of empirical data for narrow slotted finite cylinders. The information giving the effects of slot angle, slot width and cylinder length on the slot field helps to fill another gap in knowledge for finite three dimensional systems.

A final point to inject is that we have limited this paper to the discussions and measurements for E-polarized situations. A subsequent report on H-polarized radiation coupling to a narrow slotted cylinder will be issued shortly and in it many rather interesting properties will be presented.

REFERENCES

1. J. N. Bombardt & L. F. Libelo, "S.E.R.A. III. An Alternative Integral Equation with Analytic Kernels For the Slotted Cylinder Problem," HDL-TR-1588 Harry Diamond Labs., Washington, D.C., August 1972.
2. J. N. Bombardt & L. F. Libelo, "S.E.R.A. IV. Slotted Cylinders and Cylindrical Strips In the Rayleigh Limit," HDLTR-1607 Harry Diamond Labs., Washington, D.C., August 1972.
3. J. N. Bombardt & L. F. Libelo, "S.E.R.A. V. Surface Current, Tangential Aperture Electric Field and Back-Scattering Cross-Section For the Axially Slotted Cylinder at Normal, Symmetric Incidence," NSWC/WOL/TR 75-39 April 1975.
4. L. F. Libelo, A. G. Henney, J. N. Bombardt & F. S. Libelo, "S.E.R.A. X. The Axially Slotted Infinite Cylinder-Internal and Near Aperture Fields. Surface Current, Aperture Field and B.S.C.S. For Intermediate Slot Angles," NSWC/WOL/TR 75-162 January 1976.
5. A. Sommerfeld, "Partial Differential Equations in Physics," pp. 29, 159 Academic Press Inc. New York 1949.
6. P. M. Morse and H. Feshbach, "Methods of Theoretical Physics, Part II," p. 1387-1398 McGraw Hill Book Co. Inc., New York 1953.
7. Y. Hayashi, "Electromagnetic Field In a Domain Bounded by a Coaxial Circular Cylinder With Slots," Proc. Japan Acad. 40, 305 (1964).
8. Y. Hayashi, "On Some Singular Integral Equations I," Proc. Japan Acad. 40, 323 (1964).
9. R. Barakat and E. Levin, "Diffraction of Plane Electromagnetic Waves by a Perfectly Conducting Cylindrical Lamina," Jour. Opt. Soc. Amer. 54, 1089 (1964).
10. V. P. Shestopalov, "The Method of the Riemann-Hilbert Problem In the Theory of Diffraction Propagation of Electromagnetic Waves," (Untranslated from the Russian) Izd. KhGU, Kharkov (1971).
11. V. N. Koshparënok and V. P. Shestopalov, "Diffraction of a Plane Electromagnetic Wave by a Circular Cylinder with a Longitudinal Slot," Zh. Vychisl. Mat.i Mat. Fiz. 11, 721 (1971).

REFERENCES (CONT.)

12. V. N. Koshparënok, G. G. Polovnikov and V. P. Shestopalov, "Resonant Excitation of a Circular Cylinder with a Longitudinal Slot By a Plane Wave," Sov. Phys.-Tech. Phys. 17, 1630 (1973).
13. J. Stratton, "Electromagnetic Theory," Sect. 6.10, McGraw-Hill Book Co. New York, N.Y. 1941.
14. A. Erdélyi, Ed. "California Institute of Technology, Bateman Manuscript Project. Higher Transcendental Functions Vol. II," eqs. (13) and (14), p. 87, McGraw-Hill Book Co. Inc. New York, NY 1953.
15. Z. S. Agranovich, V. A. Marchenko and V. P. Shestopalov, "Diffraction of Electromagnetic Waves By Plane Metallic Gratings," Zh. tekn. Fiz. 32, No. 4, 381 (1962).
16. I. S. Gradshteyn and I. W. Ryzhik, "Tables of Integrals Series and Products," Sect. 8.91, Academic Press, N.Y., N.Y., 1965.
17. A. A. Oliner and P. B. Clarricoats, "Transverse Equivalent Networks for Slotted Inhomogeneous Circular Waveguides," Proc. of Inst. of Electrical Engin. 114, 171 (1967).
18. R. O. Dell, C. R. Carpenter and C. L. Andrews, "Optical Design of Anechoic Chambers," Jour. Opt. Soc. of America, 902, 62 (1972).
19. Textolite is the trade name of glued fibreboard rolled into cylinders. The cylinders are obtainable from General Electric Co., Schenectady, New York.
20. Aluminum Foil Scotch Tape is a standard commercial product available from 3M Company, St. Paul, Minnesota.
21. L. F. Libelo, J. P. Heckl, C. L. Andrews, D. P. Margolis. 1975 IEEE International EMC Symposium Record, Oct 1975, San Antonio, TX.
22. D. P. Margolis. Ph.D. Dissertation Department of Physics, State University of New York at Albany, N.Y. 1976.
23. S. Ramo, J. R. Whinnery and T. VanDuzer, "Fields and Waves In Communication Electronics," Section 10.08, J. Wiley & Sons, Inc., New York, 1965.